CONTROL SYSTEM FOR SHIP MODEL TOWING CARRIAGE

by

LIEUTENANT EVERETT J. LECOURT, JR., USCG

B.S., U. S. Coast Guard Academy
(1958)

SUBMITTED IN PARTIAL FULFILLMENT OF THE REQUIREMENTS

FOR THE DEGREE OF

MASTER OF SCIENCE

IN NAVAL ARCHITECTURE AND MARINE ENGINEERING

AND THE DEGREE OF

MASTER OF SCIENCE IN ELECTRICAL ENGINEERING

at the

MASSACHUSETTS INSTITUTE OF TECHNOLOGY

August, 1964

CONTROL SYSTEM FOR SHIP MODEL TOWING CARRIAGE

by

LIEUTENANT EVERETT J. LECOURT, JR., USCG

B.S., U. S. Coast Guard Academy
(1958)

SUBMITTED IN PARTIAL FULFILLMENT OF THE

REQUIREMENTS FOR THE DEGREE OF

MASTER OF SCIENCE

IN NAVAL ARCHITECTURE AND MARINE ENGINEERING

AND THE DEGREE OF

MASTER OF SCIENCE IN ELECTRICAL ENGINEERING

at the

MASSACHUSETTS INSTITUTE OF TECHNOLOGY

August, 1964

Signature of Author .....
Department of Naval Architecture and Marine Engineering, 24 August 1964

Certified by .....
Martin A. Abkowitz

.....
George C. Newton, Jr.

Accepted by .....
Chairman, Departmental Committee
on Graduate Students

CONTROL SYSTEM FOR SHIP MODEL TOWING CARRIAGE

BY

LIEUTENANT EVERETT J. LECOURT, JR., USCG

Submitted to the Department of Naval Architecture and Marine Engineering and the Department of Electrical Engineering on August 24, 1964, in partial fulfillment of the requirements for the degree of Master of Science in Naval Architecture and Marine Engineering and Master of Science in Electrical Engineering.

ABSTRACT

This thesis is a design study to determine whether or not a suitable control system for the carriage of the M. I. T. Ship Model Towing Tank can be designed using as the power element a variable speed drive—surplus from an obsolete wave generating apparatus. The drive unit, located at one end of the 108-foot tank, will pull the carriage along an overhead rail by means of a wire rope tension linkage.

The system is to operate in two modes. The first is constant speed operation. Analysis shows that the specifications for this mode can be met with an open loop system.

The second mode is to follow a model as it is towed down the tank with constant force. The feedback control system designed meets the steady-state specifications but does not meet the transient requirement because of an inherent limitation in the variable speed drive.

Failure to meet all the specifications and undesirable mechanical features cause the author to recommend not building the system.

Thesis Supervisors: Martin A. Abkowitz
Professor of Naval Architecture

George C. Newton, Jr.
Professor of Electrical Engineering

ACKNOWLEDGEMENT

The author wishes to express his appreciation to Professor Martin A. Abkowitz, Department of Naval Architecture and Marine Engineering, and Professor George C. Newton, Jr., Department of Electrical Engineering, Massachusetts Institute of Technology, for their guidance in supervising this thesis.

TABLE OF CONTENTS

TABLE OF CONTENTS cont.

LIST OF FIGURES

LIST OF TABLES

INTRODUCTION

Background

Naval architects and marine engineers have long been interested in the behavior of ships in a seaway. The measurement of ship motions in actual seas has been done for many years, and such programs are now in progress. Analytical methods have been developed to predict ship motions in waves. Another source of information is from tests of ship models. Results from these efforts have agreed in some areas, but differ widely in others[1].

Comparison of results of model tests in waves from various towing tanks have shown poor agreement[2, 3]. The discrepancies have been attributed to erratic wave generation, inaccurate measurements, and differences in testing techniques.

Experimental studies were made by Sibul[4] at the University of California to compare three methods of model testing in waves—(1) model free to heave, pitch, and surge (model towed with constant force); (2) model free to heave and pitch, but restricted in surge (model towed at constant speed); and (3) model free to heave and pitch with surge limited by soft springs. The conculsion reached as a result of this study is to use constant force towing with the model free to heave, pitch, and surge. Abkowitz makes the same recommendation based on an analytical study[5].

The M. I. T. Towing Tank Facility

The testing tank at the Massachusetts Institute of Technology is 108 feet long, 8.5 feet wide, and 4 feet deep. A falling weight dynamometer is used for constant force towing. A carriage on rails above the tank is designed for constant speed towing and to carry instrumentation for constant force towing in waves. Waves are generated by a paddle type mechanism. The paddle is driven by a hydraulic piston and is capable of generating regular and irregular waves.

Statement of the Problem

The present carriage drive does not meet the requirement of following the model while towing with constant force in waves. This has fostered interest in new approaches to the carriage control problem.

Available at the towing tank is a variable speed drive--surplus from obsolete wave generating apparatus. This thesis is a study to investigate the possibility of utilizing this variable speed drive in a carriage control system that will meet testing requirements.

II. SYSTEM SPECIFICATIONS

Testing requirements at the M. I. T. tank dictate the following specifications for the carriage control system:

1. Constant speed towing over a range of model speeds from 0.75 knots to 3.0 knots and from 3 to 12 knots with a tolerance of $\pm$ 0.5%. Load disturbances will include the fluctuating resistance of the model being towed in waves and the drag of the instrument cables leading to the recorders and indicators at one end of the tank.
2. Follow-the-model operation while towing with constant force; relative displacement limited to $\pm$ 0.5 feet.

In tests of displacement-type hulls in waves with freedom to surge, heave and pitch, the model motion of interest in design of the carriage follow-the-model control system is surge. Since the naval architect is not interested in this motion for ship design, surge (although generally recorded) is never reported with the final model-test results.

An estimate of the amplitude of surge was made by assuming a surge velocity of 15% of the average speed. For a five-foot

MARINER model towed at one knot in regular waves (wave length equal to model length; wave height equal to $\frac{1}{50}$ th of wave length), the estimated amplitude of surge is 0.38 inches at the frequency of encounter of 7.98 radians per second. This is supported by typical records reported by Paulling[6], Ben-Nun[7], and Wiener[8]. Since this is near the natural frequency of the model, this is the maximum amplitude expected. A valid input to test system performance is taken as a sinusoidal of amplitude 0.032 feet (0.38 inches) at a frequency of eight radians per second.

Tests of hydrofoil craft in waves are planned in which the boat crashes into the water from flying speed. A typical situation will be flying at approximately eight knots and crashing to a final speed of about three knots--a step change in speed of five knots (8.45 feet per sec). The control system must maintain the relative displacement between carriage center and model less than one foot. This requirement is necessary to keep the dolly which is attached to the model and riding on a track within the carriage, from hitting positive stops.

III. DESCRIPTION OF THE SYSTEM

General Description

The variable speed drive will be used to pull the carriage along its rails by means of a wire rope tension linkage. This is shown schematically in Figure 1.

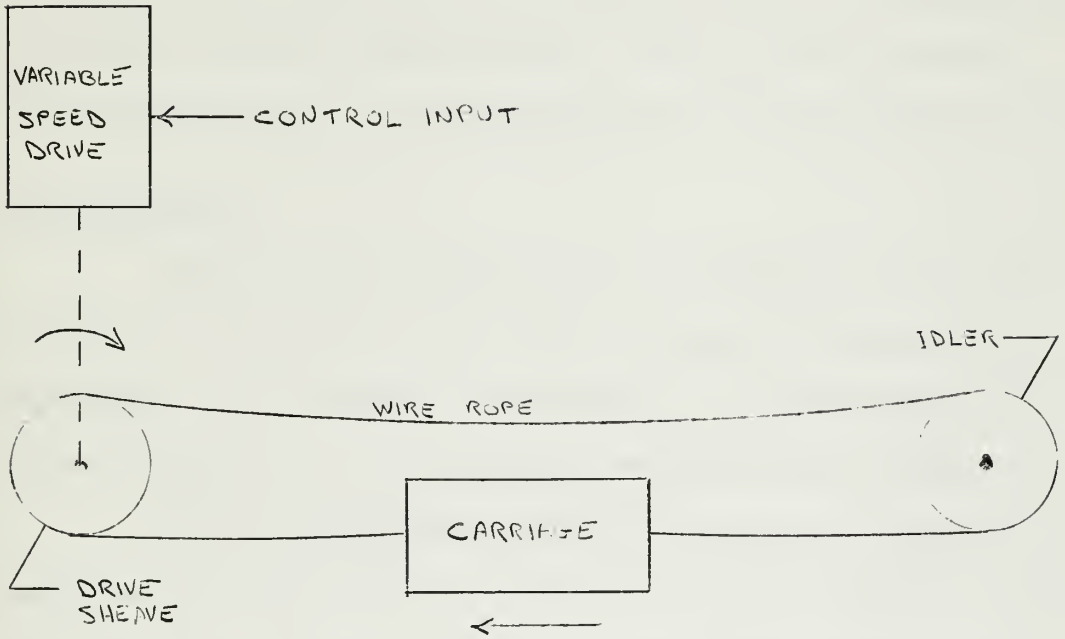

Figure 1
System Schematic

The variable speed drive (driven by a three-phase induction motor) has an output range from 31.5 RPM to 126 RPM. With a diameter of 0.385 feet for the drive sheave and direct coupling, the speed range of the carriage will be from 0.75 to 3.0 knots. For high speed, a step-up gear ratio of 4:1 will give a speed range of 3.0 to 12. knots. These ranges correspond to those given in the system specifications.

Starting and stopping will be done manually (limit switches can also be provided). The starting transient of the induction motor will provide acceleration of the carriage and model. Braking will be necessary to reduce stopping distance. Reversing can be easily accomplished by using a reversing controller for the induction motor.

Towing Carriage

The carriage is supported by an overhead rail and a rail located on the side wall. The sketch of Figure 2 illustrates this arrangement. The weights of the carriage and its attachments are given in Appendix A. For design purposes a mass of ten slugs was used.

The friction properties of the carriage were determined by measuring the force required to move the carriage at constant speeds. Data show coulomb friction of approximately fifteen pounds and viscous friction of 0.5 pound per knot (0.296 pound-second per foot). See Figure 3.

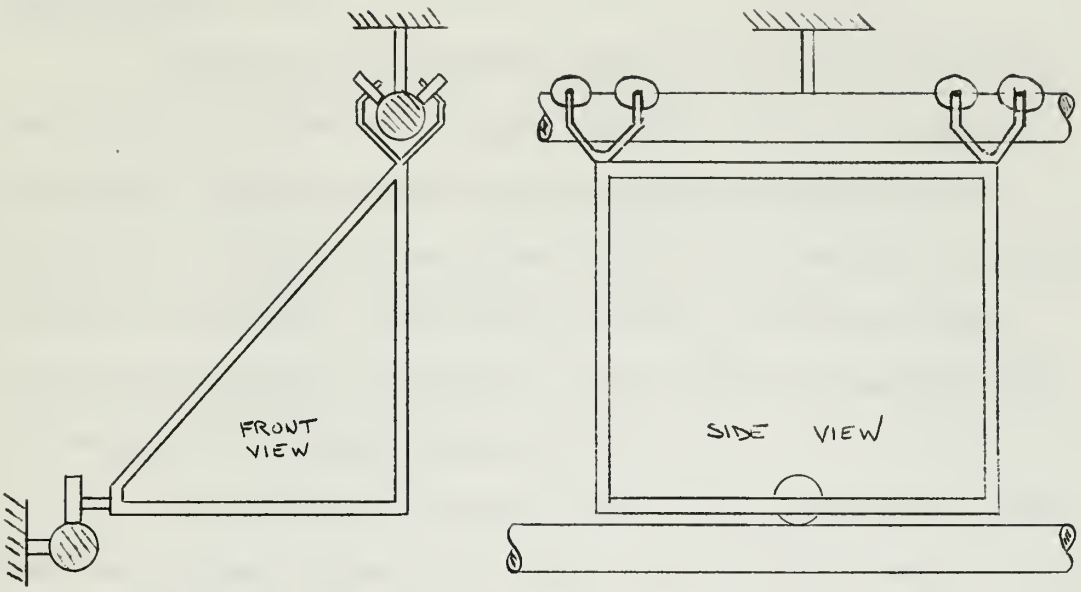

Figure 2

Carriage

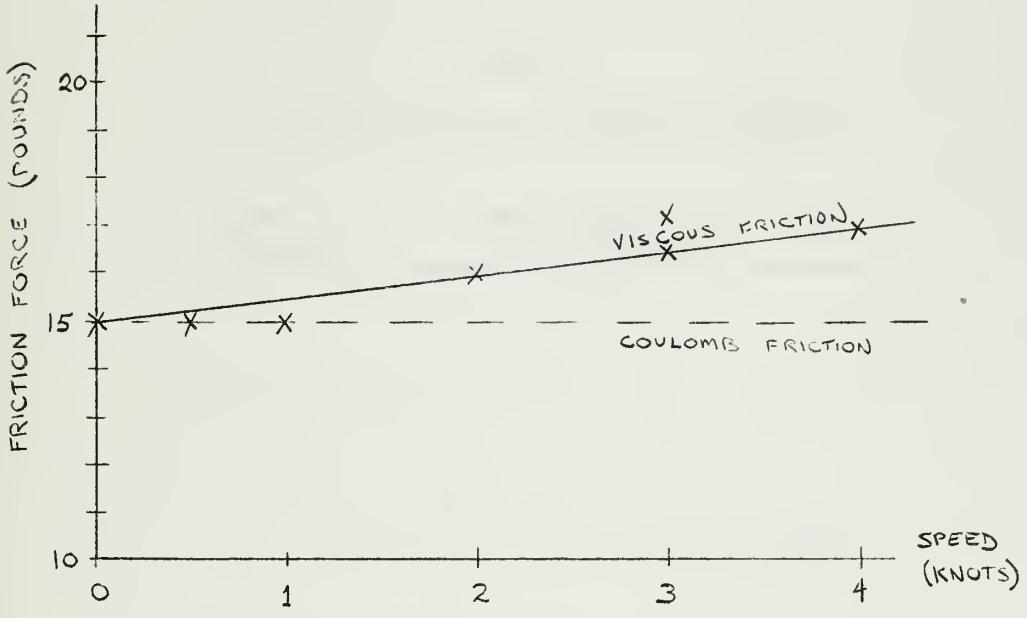

Figure 3

Friction Properties of Carriage

Cable Slides

Cables from transducers located on the model and carriage are led to indicators at one end of the tank. They are supported along their 100-foot length by fifteen slides riding on an overhead rail. The force to move these slides is a function of position as well as velocity. At the start of a run, the force is small; at the end, the force is maximum. Table 1 gives the maximum value at the end of the run at several speeds.

The slides for the power cables to the drive motor on the carriage (present system) have similar characteristics and are listed in Table 2. These cables would not be used with the system under design and could be disconnected, eliminating this disturbance. This is assumed to be the case in the following analysis.

Table 1

Friction Forces of Instrument Cables

Speed (knots)	Max. Force at End of Run (pounds)
1	12
2	13
3	15

Table 2

Friction Forces of Power Cables

Speed (knots)	Max. Force at End of Run (pounds)
1	30
2	32
3	36

Wire Rope Transmission

For pulling the carriage along, both wire rope and roller chain were investigated. Wire rope proved to be superior from consideration of weight, strength, and elastic properties.

The wire rope can be modeled as a massless spring, the mass of the wire being less than 10% of the mass of the carriage. The equivalent spring constant of the transmission will be that due to the elastic properties of the wire in series with that due to the catenary.

The elastic spring constant is given by

$$k_e = \frac{EA}{\ell}$$

where k_e is the spring constant
ℓ is the length of wire
E is the modulus of elasticity,

and A is the cross-sectional area. Values of "EA" determined from the actual test data is available from the wire rope manufacturer[9].

The spring effect due to the cantenary can be treated analytically. If the shape of the catenary is approximated by a parabola (extremely close approximation when sag is small, as in this application), an incremental linear model yield the relation

$$k_c \approx \frac{12\, H_0^3}{w^2\, \ell_0^3}$$

where k_c is the spring constant,
H_0 is the horizontal component of the steady-state tension,
w is the weight of the wire per foot,
and ℓ_0 is the steady-state length of the span.

Development of the above relation, the details of wire rope selection, and comparison of wire rope and roller chain appear in Appendix B.

The expressions above show that the spring constant is dependent on the position of the carriage. The spring constant is smallest at the start position and increases as the carriage moves down the tank (See Appendix B). System performance will, therefore,

improve as the natural frequency of the transmission increases. For this reason the spring constant is taken as 20,000 pounds per foot (corresponding to a carriage position just after starting) and is considered to be constant for design purposes.

Transmission Transfer Function

The sketch of the system in Figure 4 shows the following:

θ_D - position of the drive sheave

x_c - position of the carriage

H_1 - tension in wire from the carriage to the drive sheave

H_2 - tension in wire from the drive sheave, over the idler, and back to the carriage

k_1 - spring constant of wire 1

k_2 - spring constant of wire 2

R_D - radius of drive sheave

M_c - mass of the carriage

F_c - coulomb friction of carriage

f_c - viscous friction of carriage

L - load on the carriage from ship model, cable drag, etc.

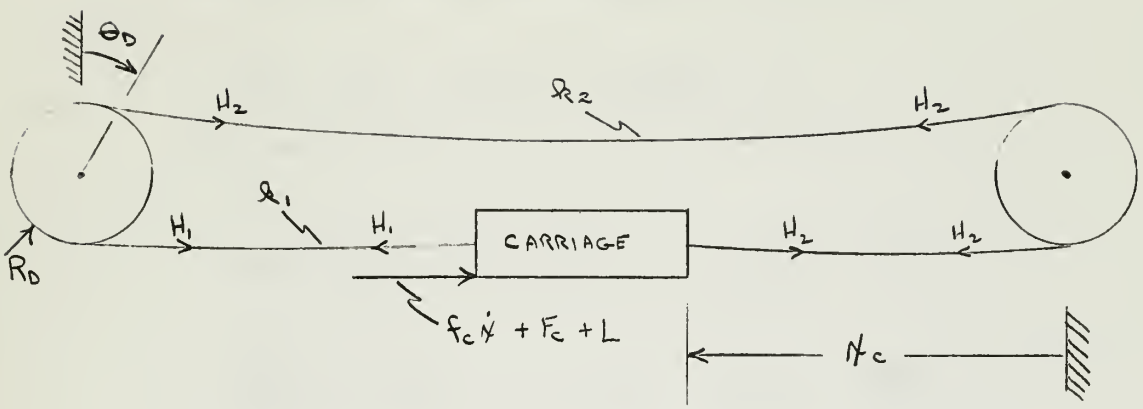

Figure 4

System Force Diagram

Writing the force equation for the carriage yields

$$H_1 - H_2 = M_c\ddot{x}_c + f_c\dot{x}_c + F_c + L$$

The tension in each spring is, respectively,

$$H_1 = H_0 + k_1(R_D\theta_D - x_c)$$

$$H_2 = H_0 - k_2(R_D\theta_D - x_c)$$

$$H_1 - H_2 = k_{eq}(R_D\theta_D - x_c)$$

where $k_{eq} = k_1 + k_2$.

Substituting in the force equation gives

$$M_c\ddot{x}_c + f_c\dot{x}_c + k_{eq}x_c = k_{eq}R_D\theta_D - F_c - L.$$

Taking the time derivative gives

$$M_c \dddot{x}_c + f_c \ddot{x}_c + k_{eq} \dot{x}_c = k_{eq} R_D \dot{\theta}_D - \dot{L}.$$

The transform is

$$(M_c S^2 + f_c S + k_{eq})\, \dot{x}_c(S) = k_{eq} R_D \dot{\theta}_D(S) - \dot{L}(S)$$

$$\left(\frac{M_c}{k_{eq}} S^2 + \frac{f_c}{k_{eq}} S + 1\right) \dot{x}_c(S) = R_D \dot{\theta}_D(S) - \frac{\dot{L}(S)}{k_{eq}} \quad .$$

For M_c = 10 slugs, k_{eq} = 20,000 pounds per foot, and f_c = 0.296 pound-second per foot, the natural frequency is 44.7 radians per second and the damping ratio is 3.3×10^{-4}. This low damping ratio is undesirable. If the viscous damping of the carriage is increased to the maximum allowed by full-load rating of the Link-Belt drive at a carriage speed of 12 knots, the damping ratio is increased to 0.00615. This corresponds to a value of f_c equal to 5.5 pounds-sec per foot (9.25 pounds per knot). This can easily be accomplished by the addition of a mechanical device to the carriage which exhibits the desired viscous friction.

IV. DESCRIPTION OF THE VARIABLE SPEED DRIVE

Link-Belt P.I.V. Drive

The variable speed unit is the Link-Belt P.I.V. drive with a speed ratio of 4:1 (Name plate data are listed in Appendix C). The input shaft is driven at nearly constant speed (875 RPM) by a three phase induction motor through 2:1 reduction gears. The speed ratio of the output shaft to the input shaft can be varied between 2:1 and 1:2. The output is then transmitted through a 13.9:1 double reduction gear train, giving a range of speed from 126 to 31.5 RPM. (See schematic in Figure 5).

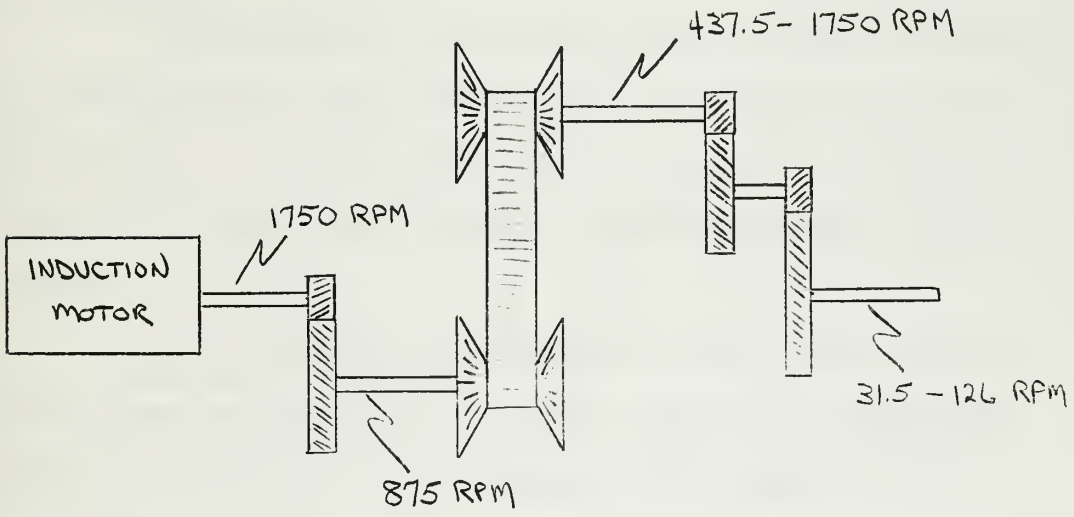

Figure 5
Schematic of Link-Belt P.I.V. Drive

The Link-Belt unit employs a positive, chain drive. The chain is self-tooth forming and engages radial grooves in two pairs of cone-shaped wheels. The wheels of each pair, mounted on splined shafts, can be moved together or apart by turning a control screw. As the conical surfaces are moved together on one shaft, the chain walks out along the grooves, effectively increasing the diameter of this sprocket. At the same time the cones on the other shaft are moved apart; the effective diameter of the sprocket being reduced. The ratio of the speeds of the two shafts can thus be changed steplessly from 2:1 to 1:2. This is illustrated diagrammatically in Figure 6.

Control Input

Speed changes in the Link-Belt drive are made by turning the control screw. The no-load output shaft speed versus control screw position is plotted in the graph of Figure 7. Sixteen revolutions of the control screw cover the output speed range of 31.5 to 126 RPM.

The torque-speed characteristic of the control screw as given by the manufacturer[10] is shown in Figure 8. Because the chain walks along the conical surfaces as the control screw is turned, there is a limit on the rate at which speed changes can be made. The practical limit is 380 RPM. An approximate model for this

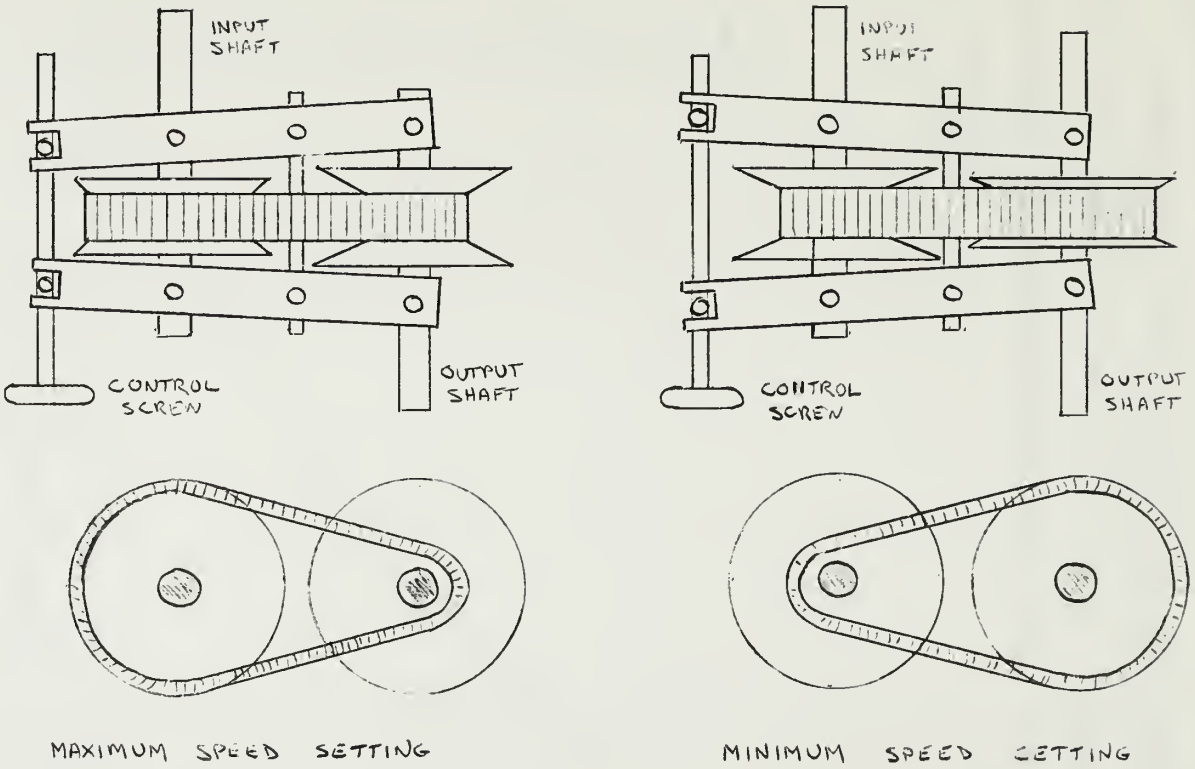

Figure 6

Action of Control Screw in Changing Speed Ratio

characteristic is taken as a linear relation with a limit on the velocity. This is shown on the graph of Figure 8 as a dashed line.

Induction Motor

The variable speed unit is driven by a three-phase induction motor rated at 5 horsepower at 1750 RPM (name plate listed in Appendix C). The torque-speed characteristic of this motor is shown in Figure 9.

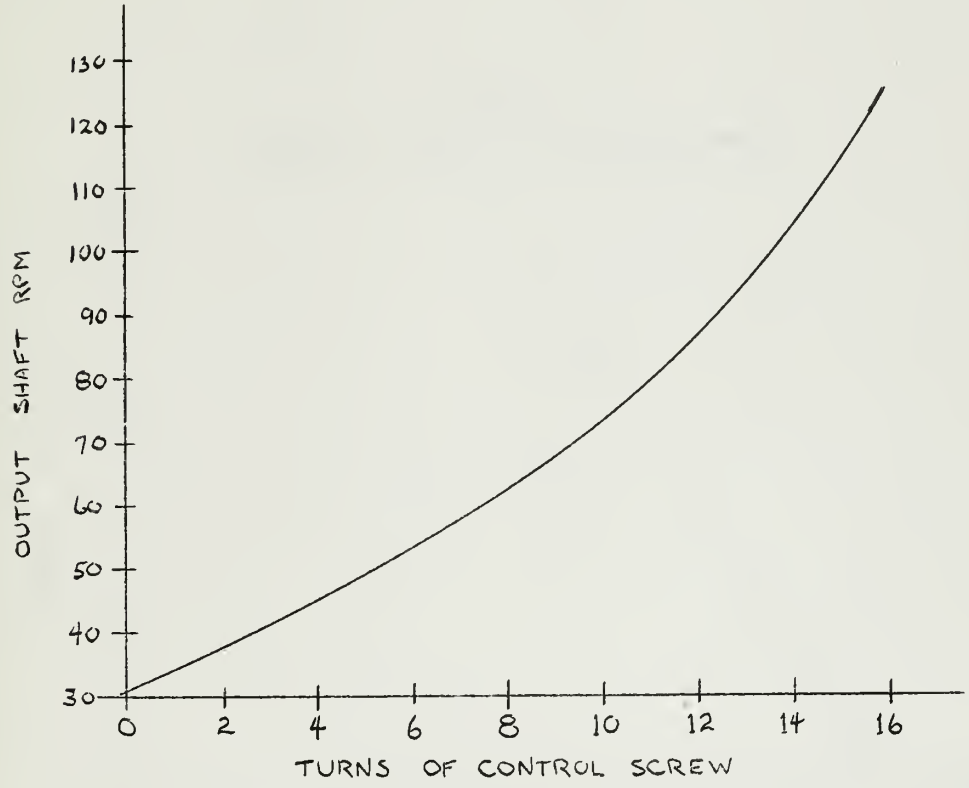

Figure 7
Output Shaft Speed vs. Control Screw Position

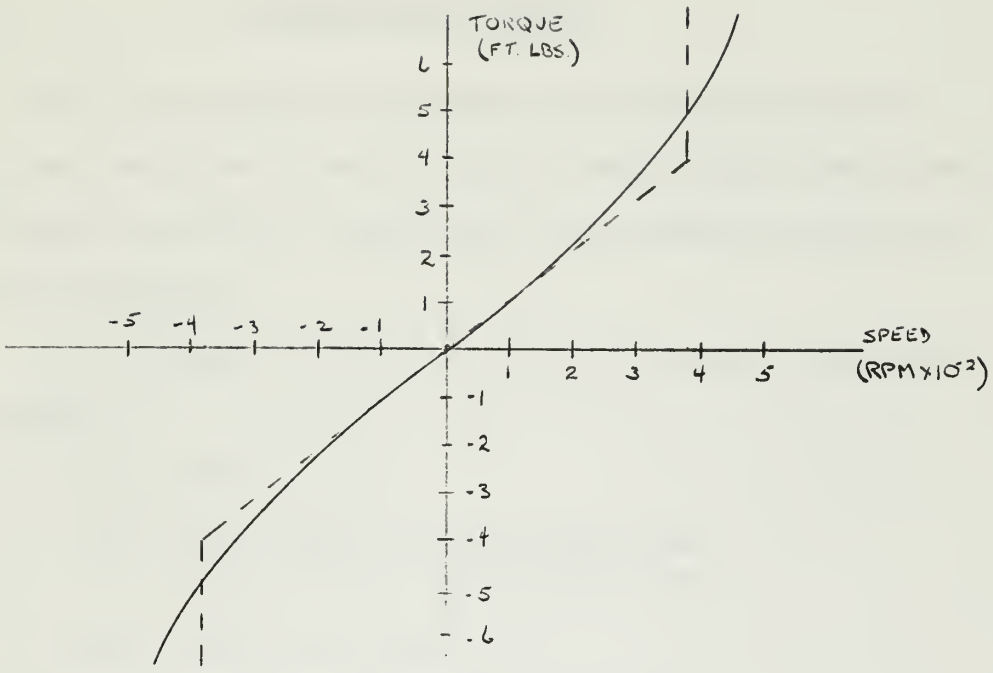

Figure 8

Torque vs. Speed for Control Screw

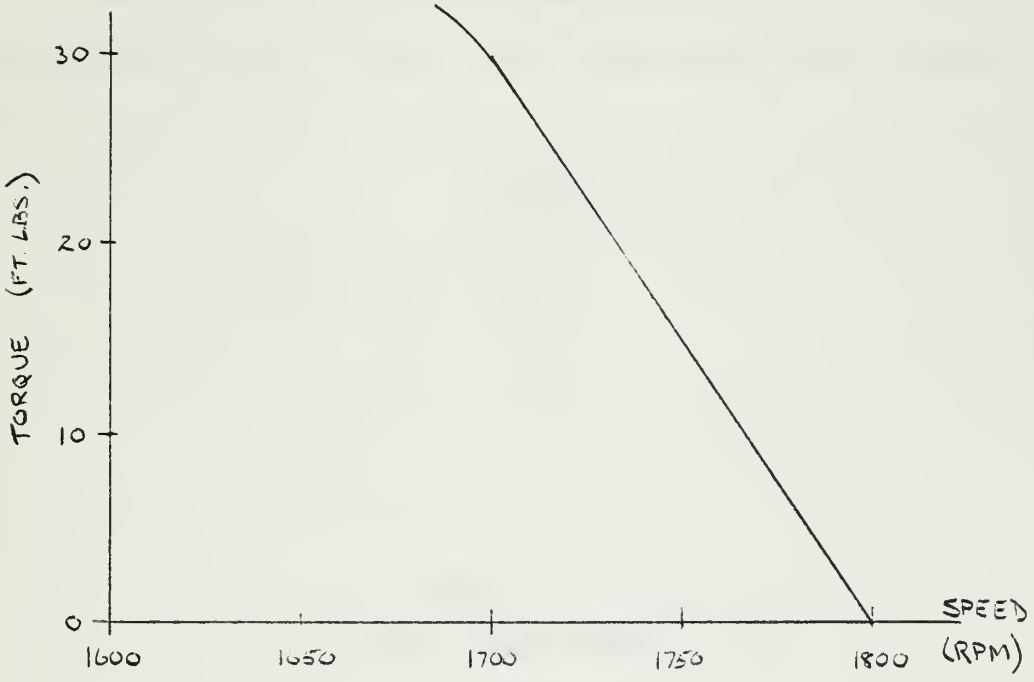

Figure 9

Torque-Speed Characteristic of Induction Motor at Rated Voltage

V. CONSTANT SPEED TOWING

The specifications for constant speed towing can be met with an open loop system. This is evident from a study of the dynamics of the variable speed drive and the wire rope transmission system for given load disturbances.

An incremental linear model of the drive unit is shown in Figure 10 where

J_D is the inertia

B_D is the negative of the slope of the induction motor torque-speed curve,

ω_D is shaft velocity

R_D is the diameter of the drive sheave,

and L is the load disturbance (force),

all quantities being referred to the output shaft of the Link-Belt unit.

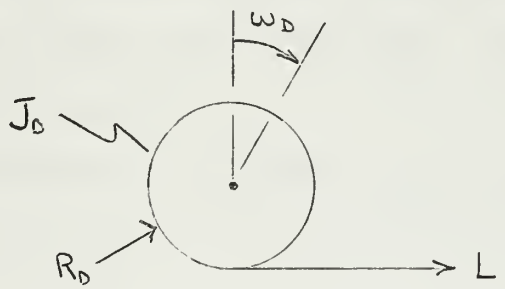

Figure 10
Model of Drive Unit

Applying Newton's second law,

$$- R_D L - B_D \omega_D = J_D \dot{\omega}_D,$$

$$- R_D L = J_D \dot{\omega}_D + B_D \omega_D$$

$$- R_D L = B_D \left(\frac{J_D}{B_D} S + 1\right) \omega_D .$$

In the low speed range (0.75 to 3.0 knots) the allowable carriage velocity error is $\pm$ 0.005 knots ($\pm$ 0.008 feet per second) which corresponds to $\pm$ 0.0208 radian per seconds of the drive shaft.

The value of B_D is 0.3 foot-pounds per RPM (2.87 foot-pounds-second per radian), the negative of the slope of the torque-speed characteristic of Figure 9, multiplied by the square of the effective gear ratio.

The inertia J_D varies from 95.5 slug-feet^2 at 31.5 RPM to 6.25 slug-feet^2 at 126 RPM. For 31.5 RPM, $\frac{B_D}{J_D}$ = 98 seconds^{-1}; for 126 RPM, $\frac{B_D}{J}$ = 94 seconds^{-1}.

At low frequencies, the largest sinusoidal load disturbance that can be tolerated will be

$$|L| = \frac{B_D}{R_D} \omega_D$$

$$|L| = \frac{2.87}{.385} \left(\frac{1800}{126}\right)^2 0.0208$$

$$|L| = 31.6 \text{ pounds}$$

This is well above the disturbance load from a model towed in waves which would be only a fraction of a pound. It is also seen that the drag of the instrument cables will not cause a speed drop exceeding that allowed by the specifications.

In high speed operation, the effective diameter of the drive sheave R_D is increased by a factor of 4; but the allowable error is also increased by the same amount, so that above analysis is valid for both high and low speed ranges. The induction motor speed can, therefore, be considered constant at an operating point determined by the steady-state load.

The motion of the carriage for load disturbances can be studied using the model shown schematically in Figure 11.

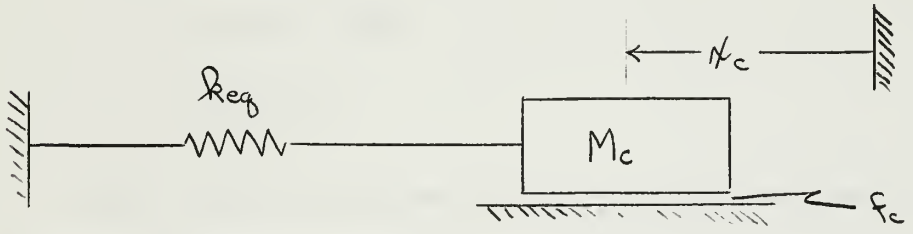

Figure 11
Model of Carriage and Transmission System

The equation of motion for this system is

$$L = M_c \ddot{x}_c + f_c \dot{x}_c + k_{eq} x_c$$

$$L = k_{eq}\left(\frac{M_c}{k_{eq}} S^2 + \frac{f_c}{k_{eq}} S + 1\right) x_c$$

$$x_c = \frac{L}{k_{eq}\left(\frac{M_c}{k_{eq}} S^2 + \frac{f_c}{k_{eq}} S + 1\right)}$$

At the frequency of the test input (8 radians per second) described in Section II, the magnitude of the allowable disturbance for a velocity error less than $\pm$ .008 feet per second is approximately

$$L = k_{eq} x_c$$

$$L = 20{,}000 \times \frac{.008}{8}$$

$$L = 20 \text{ pounds}$$

Again this is considerably less than the fraction of a pound expected in model tests.

What value of a step load could be tolerated? Since the system is so lightly damped, the step response will be almost a sinusoidal oscillation at the natural frequency of 44.7 radians per

second with an overshoot very nearly one. Using the same approach as above,

$$L = k_{eq} x_c$$

$$L = 20{,}000 \times \frac{.008}{44.7}$$

$$L = 3.6 \text{ pounds}$$

The disturbance from the instrument cables described in Section III can be modeled as fifteen successive step increases of one pound each. It is seen that the error from these disturbances will not exceed that allowed by the specifications.

The conclusions that can be drawn from the above study are:

1. the induction motor can be treated as a constant speed device about an operating point and
2. the specifications for constant speed towing can be met with an open loop system (Figure 12).

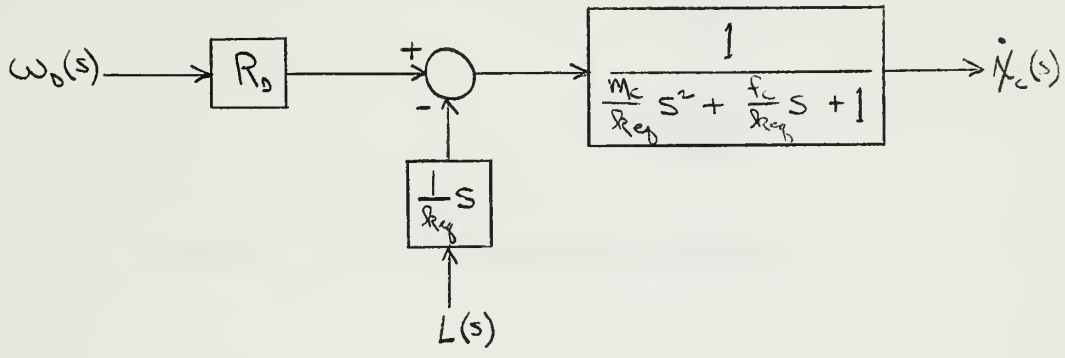

Figure 12
Block Diagram of Open Loop System for Constant Speed Towing

VI. FOLLOW-THE-MODEL SYSTEM

Description of the System

The actuating signal in the follow-the-model system will be the relative position between the mid-point on the carriage and the midship section of the model. An amplifier will drive a DC servo motor to position the control screw, controlling the output speed of the Link-Belt drive. The carriage is pulled by the drive through the wire rope transmission. This is shown schematically in Figure 13.

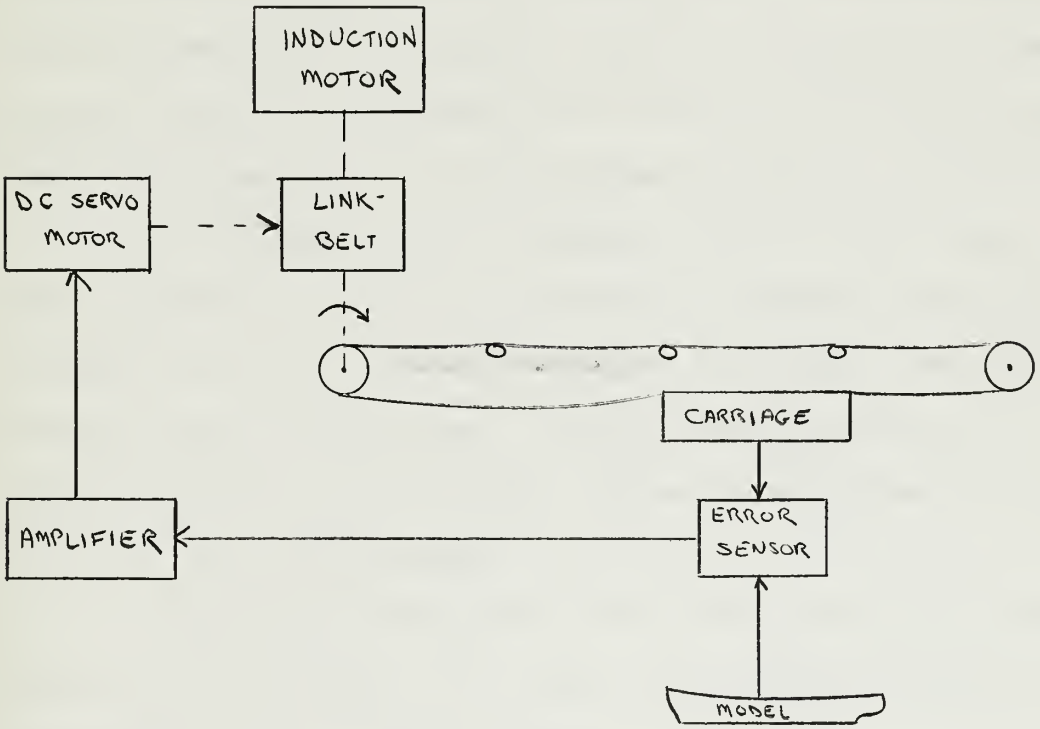

Figure 13
Schematic of the Follow-the-Model System

There are several problems which are immediately evident. One is that of getting the system going. Before the start of a test run, the induction motor is necessarily stopped. To get the model moving, the falling weight of the dynamometer must be released; to get the carriage moving, the induction motor must be started. An easy method of coordinating these two operations is to fix the model (in surge) to the carriage and utilize the starting transient of the induction motor to accelerate the model to near its final average speed. When this transient is completed, the model can be released and the follow-the-model system activated. This can be accomplished mechanically by using a pin to hold the model at the center of the carriage during the accelerating period, and then lifting the pin with a solenoid.

The second problem is stopping at the end of the tank. Limit switches can be used to de-energize the induction motor and set a brake on the drive. The model will then drift ahead, hitting the positive stops on the carriage. The impact will be softened by buffers installed on the carriage. Both model and carriage will come to rest at the end of the tank.

The return of the model to the starting point can be done with the open loop system. The model is then prepared for another run by setting the pin to restrict surge.

Description of Components

The error sensor will give a voltage proportional to the relative distance between the ship model and the carriage. If x_S and x_c are the distance of the ship and carriage, respectively, measured from a fixed reference, then the error voltage e is given by

$$e = k_L(x_S - x_c)$$

where k_L is the constant of proportionality.

The DC servo motor selected for the control screw drive motor is a General Electric, 4-pole, permanent magnetic field, 1/4 horsepower motor. The selection procedure outlined by Newton[11] was followed, the details appearing in Appendix D. A full description of the motor selected also appears in this appears in this appendix.

An SCR (silicon controlled rectifier) power amplifier was selected to drive the control screw motor. The detailed circuit design was not carried out, but a good description of such an amplifier was taken from Gibson and Tuteur's analysis of a thyratron amplifier[12].

A simple circuit giving bidirectional control is shown in Figure 14. The supply is a 120 VAC, 60 cycle per second. The SCR's do not conduct until they are gated, then they conduct for the remaining portion of that half cycle. One SCR is capable of conducting during

the positive half-cycle, driving the motor in the forward direction. The second SCR conducts during the negative half cycle, driving the motor in the reverse direction. At near zero speeds, both SCR's conduct for a small portion of its half cycle. This provision is necessary to eliminate a dead zone that would exist in switching from one SCR to the other if only one is allowed to conduct.

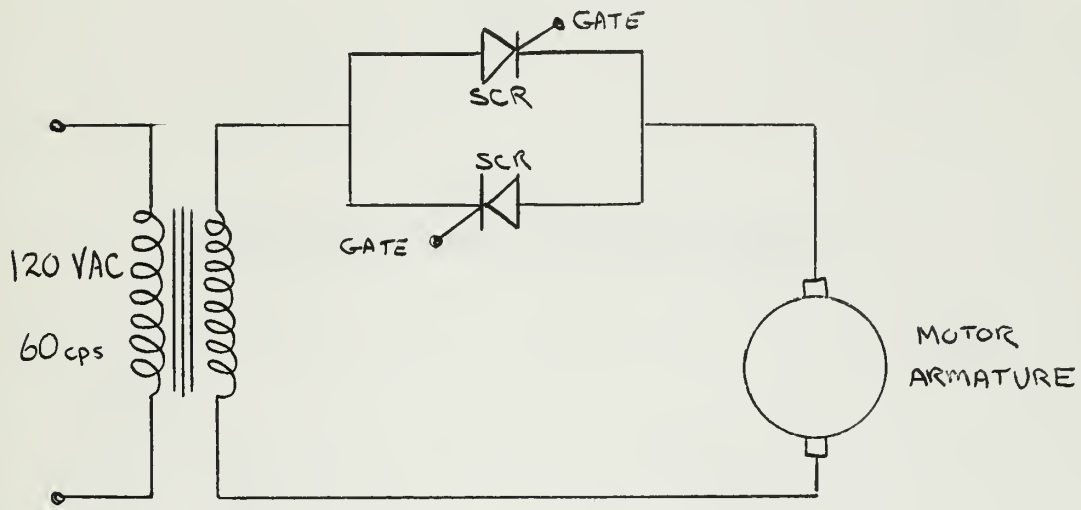

Figure 14
SCR Amplifier Circuit

The output wave form for zero control signal is shown in Figure 15. A positive control signal advances the firing point on the positive half cycle and retards the firing point on the negative half cycle. This is illustrated in Figure 16. For a negative control signal the action is reversed.

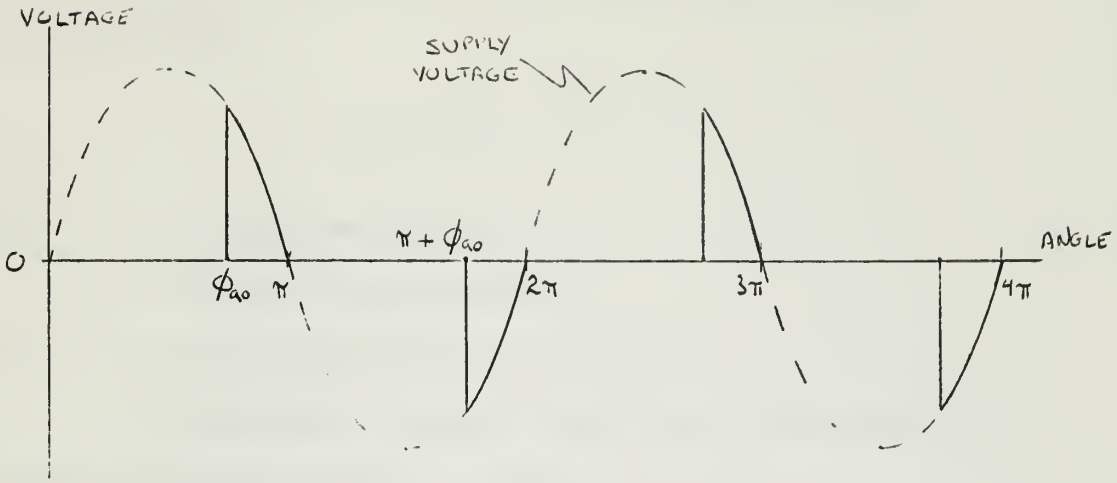

Figure 15

Voltage Wave Form at Zero Control Signal

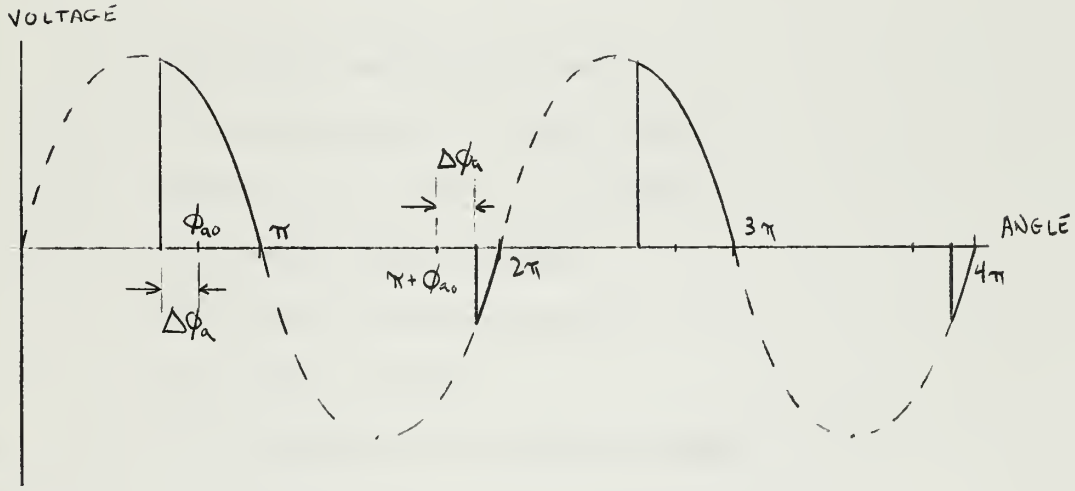

Figure 16

Voltage Wave Form for Positive Control Signal

The developed torque of a DC motor with a constant field is given by

$$Q_d = k_t I$$

where I is the armature current

k_t is the motor torque constant

and Q_d is the torque developed by the motor.

By averaging the armature current over a full cycle and using the expression above, the average torque is

$$Q_d = \frac{k_t}{\pi R_a} \left[E_s \sin\varphi_{ao} \sin \Delta\varphi_a - k_v \Omega(\pi - \varphi_{ao}) \right]$$

for $-\frac{\pi}{4} \leq \Delta\varphi_a \leq \frac{\pi}{4}$,

where R_a is the motor amature resistance,

φ_{ao} is the firing angle for zero signal,

$\Delta\varphi_a$ is the advance of the firing angle,

k_t is the motor torque constant,

k_v is the motor voltage constant,

Ω is the motor velocity

and E_s is the amplitude of the supply voltage.

This expression neglects armature inductance which, for the servo motor selected, is small.

For $\varphi_{ao} = \frac{3\pi}{4}$ and $.707E_s = 120$ volts, the above expression reduces to

$$\varphi_d = \frac{k_t}{\pi R_a} \left[120 \sin \Delta\varphi_a - \frac{\pi k_v}{4} \Omega \right]$$

$$\varphi_d = \frac{120 k_t}{\pi R_a} \sin \Delta\varphi_a - \frac{k_t k_v}{4R_a} \Omega$$

The slope of the torque-speed curve of the motor drive by this amplifier will be

$$\frac{dQ_d}{d\Omega} = - \frac{k_t k_v}{4R_a} .$$

This is the same as a linear DC motor with the armature resistance equal to $4R_a$.

Near the ends of the range $-\frac{\pi}{4} \leq \Delta\varphi_a \leq \frac{\pi}{4}$ the amplifier begins to saturate, and beyond this interval saturation is pronounced. The equivalent output voltage versus firing angle is plotted in Figure 17, showing actual saturation with a 120 VAC supply. The piecewise linear approximation used for design purposes is shown as a dashed line in the same figure.

Using the piecewise linear model, the torque relationship is

$$Q_d = \frac{120\ k_t}{\pi R_a} \Delta\varphi_a - \frac{k_t k_v}{4R_a} \Omega$$

for $-1 \leq \Delta\varphi_a \leq 1$.

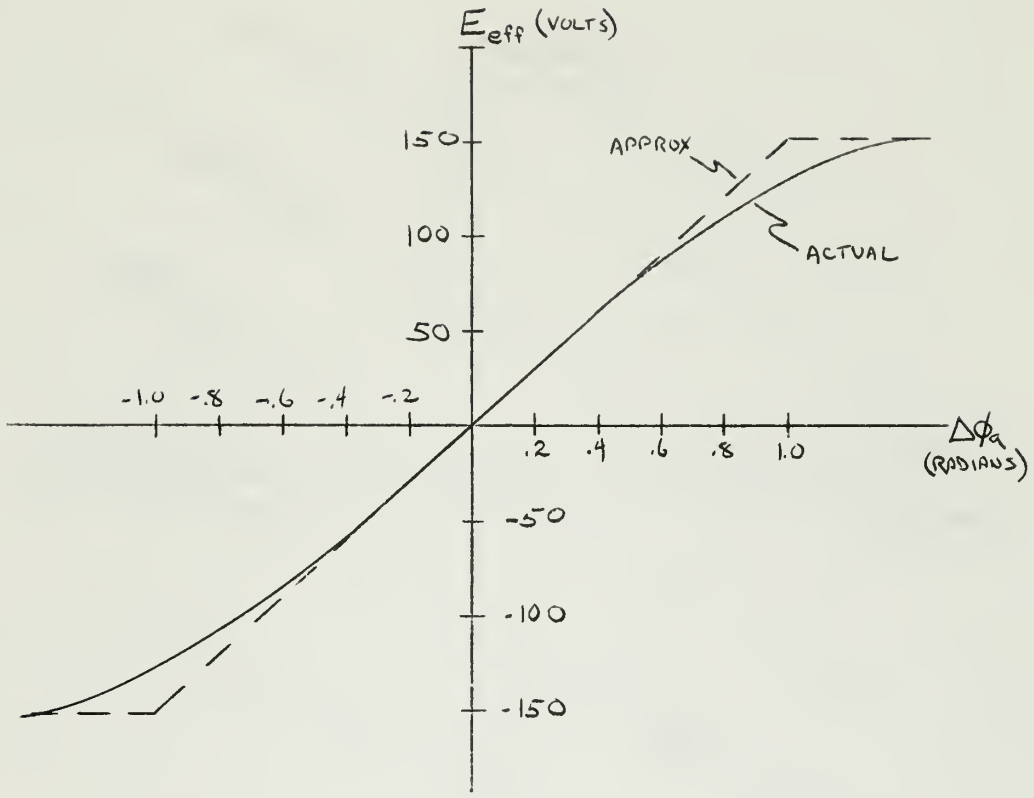

Figure 17

Effective Voltage of SCR Amplifier vs. Firing Angle

The amplifier saturation has been adjusted so that at a motor speed of 80 radians per second the motor develops 2 foot-pounds of torque which corresponds to the driving requirements of the control screw (4-foot-pounds at 40 radians per second) when driven through a 2:1 reduction gear. This has been illustrated in Figure 18, where the developed torque versus speed of the motor (reflected through the reduction gear) is superimposed on the required torque-speed of the control screw.

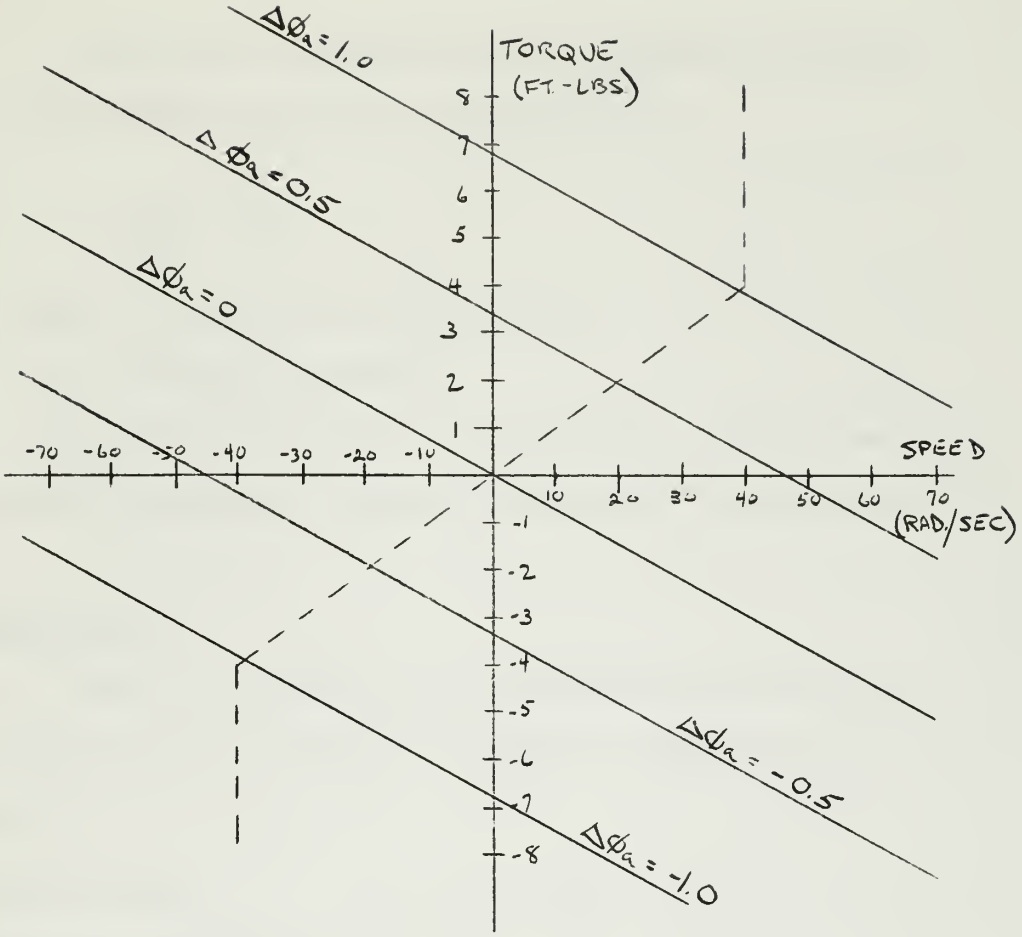

Figure 18

Developed Torque-Speed of Motor Superimposed on Required Torque-Speed of the Control Screw

Thus, the system will always operate in the linear region of the torque-speed requirement of the control screw, and the only non-linear element in the region is the saturating amplifier.

The firing of the SCR's can be controlled by a linear phase shift network which can be represented as

$$\Delta\varphi_a = k_\varphi e$$

where $\Delta\varphi_a$ is the advance in firing angle

e is the error voltage

and k_φ is the constant of proportionality. Such a network is described in the General Electric SCR Handbook[13] and by Cantor[14].

System Analysis

The block diagram for the system can now be developed. The relations for the various components are repeated here for convenience:

Error sensor, $e = k_L (x_S - x_c)$

Phase shift network, $\Delta\varphi_a = k_\varphi e$

Torque relationship, $Q_d = \frac{120\, k_t}{\pi R_a} \Delta\varphi_a - \frac{k_t k_v}{4R_a} N_B \dot{\theta}_B$.

The dynamic relation between the control screw and the control motor is

$$Q_d = (J_m + \frac{J_L}{N_B^2}) N_B \ddot{\theta}_B + \frac{B}{N_B^2} N_B \dot{\theta}_B .$$

where J_m is the inertia of the motor

J_L is the inertia of the control screw

B is the slope of the torque-speed curve of the DC Motor

N_B is the gear ratio

θ_B is the position of the control screw.

Taking the transform yields

$$\frac{Q_d}{N_B} = S\left[\left(J_m + \frac{J_L}{N_B^2}\right) S + \frac{B}{N_B^2}\right] \theta_B$$

$$\theta_B = \frac{\frac{Q_d}{N_B}}{S\left[\left(J_m + \frac{J_L}{N_B^2}\right) S + \frac{B}{N_B^2}\right]} \quad .$$

Section V showed that the Link-Belt induction motor can be treated as a constant speed device at a speed determined by the steady-state load. The linear, incremental model about a steady-state output speed can then be represented by

$$\omega_D = K_B \theta_B$$

where K_B is the slope of the curve in Figure 7 of Section IV at the operating point speed.

The transfer function of the wire rope transmission was developed in Section III and is repeated here.

$$x_c = \frac{1}{S\left(\frac{M_c}{k_{eq}} S^2 + \frac{f_c}{k_{eq}} S + 1\right)} \left(R_D \omega_D - \frac{\dot{L}}{k_{eq}}\right)$$

The block diagram is drawn in Figure 19 and reduced to that in Figure 20, where

$G_c(S)$ is cascade compensation,

$$\alpha = \frac{B}{N_B^2} + \frac{k_t k_v}{4R_a}$$

$$J = J_m + \frac{J_L}{N_B^2}$$

and

$$K = \frac{120\, k_L k_\varphi k_t K_B R_D}{\pi R_a N_B \alpha}$$

The numerical values for the parameters are:

$$J = .00108 + \frac{6.82 \times 10^{-6}}{4} \approx .00108 \text{ slug-feet}^2$$

$$\alpha = \frac{.1}{4} + \frac{.6 \times .83}{4 \times 6.8} = .0433 \text{ foot-pound-second}$$

$$\frac{J}{\alpha} = \frac{.00108}{.0433} = .025 \text{ seconds}$$

k_{eq} = 20,000 pounds per foot

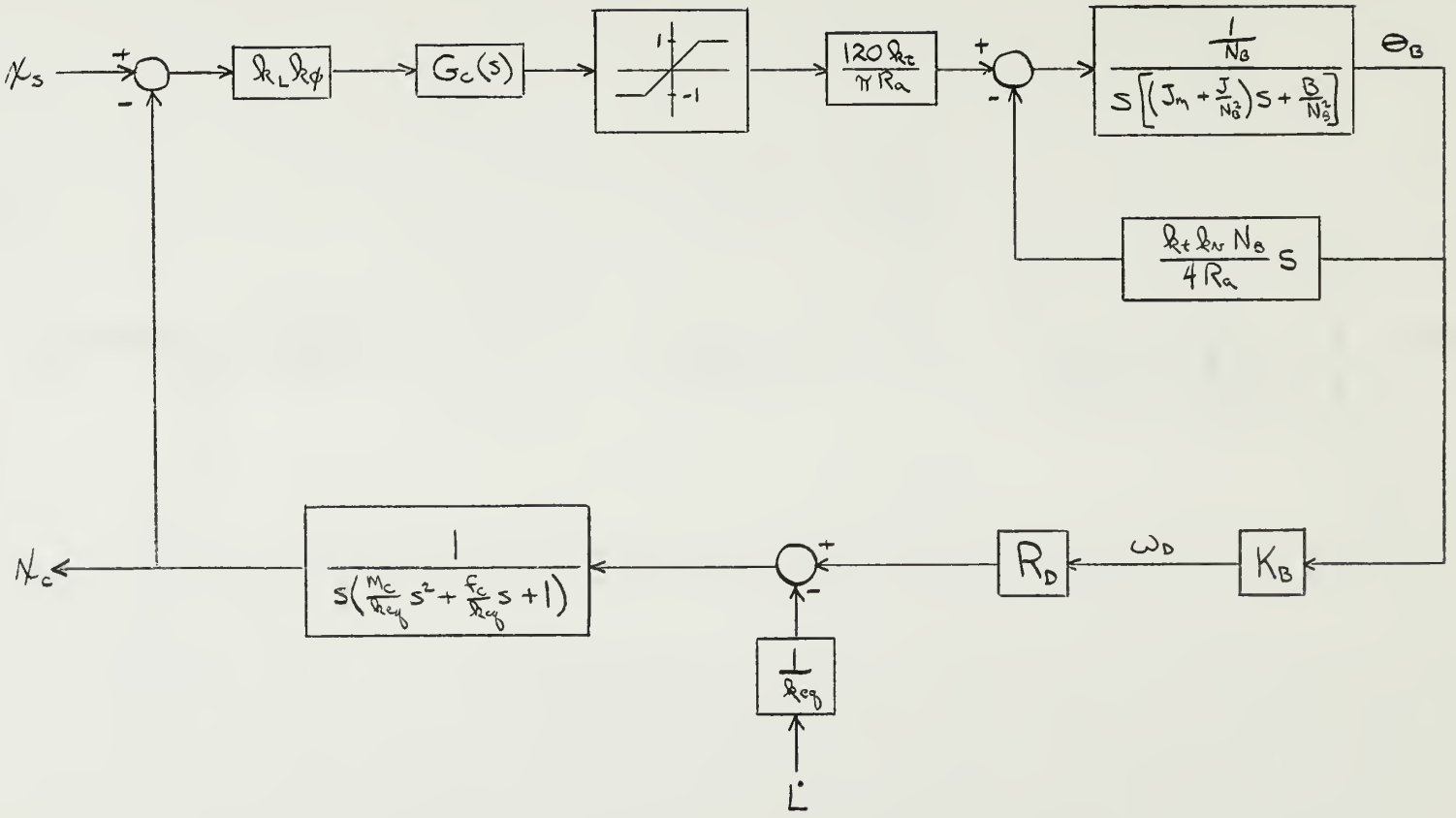

Figure 19

Block Diagram of the Follow-the-Model System

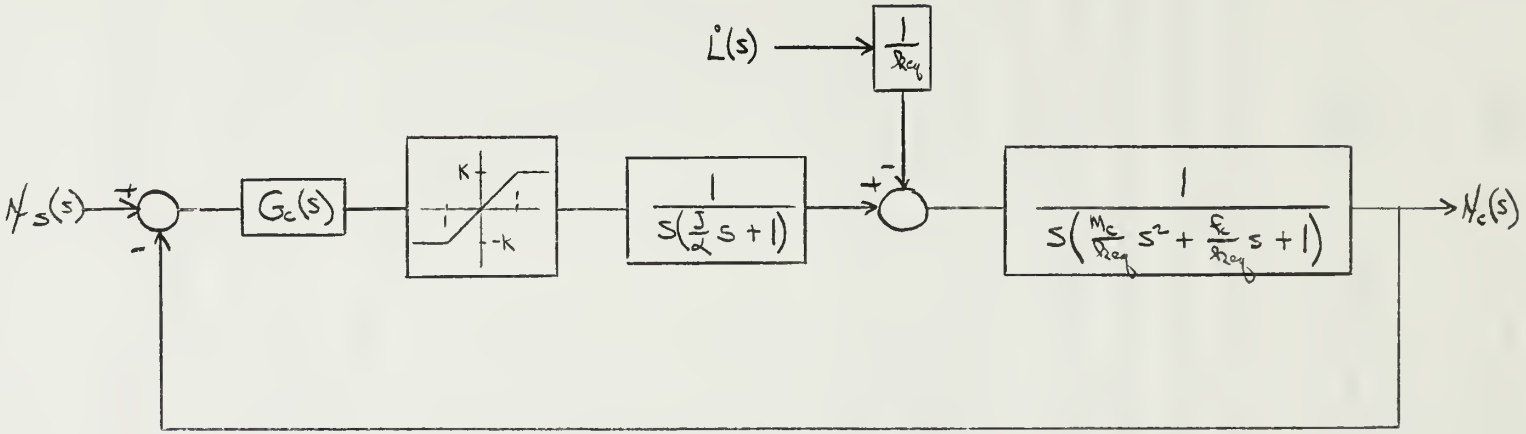

Figure 20

Reduced Block Diagram

$$\frac{M_c}{k_{eq}} = \frac{10}{20000} = .0005 \text{ seconds}^2$$

$$\frac{f_c}{k_{eq}} = \frac{5.5}{20000} = .000275 \text{ seconds}$$

Since the saturating element (frequency independent) is the only non-linear element in the system as modeled, a stability analysis can be made utilizing the describing function technique. Compensation of the system can then be performed in a manner similar to that used in linear system analysis[15, 16].

The describing function N(A) for the saturating element is shown in Figure 21, where A is the amplitude of a sinusoidal input to the element and N(A) is the effective gain for the fundamental component of the output[15].

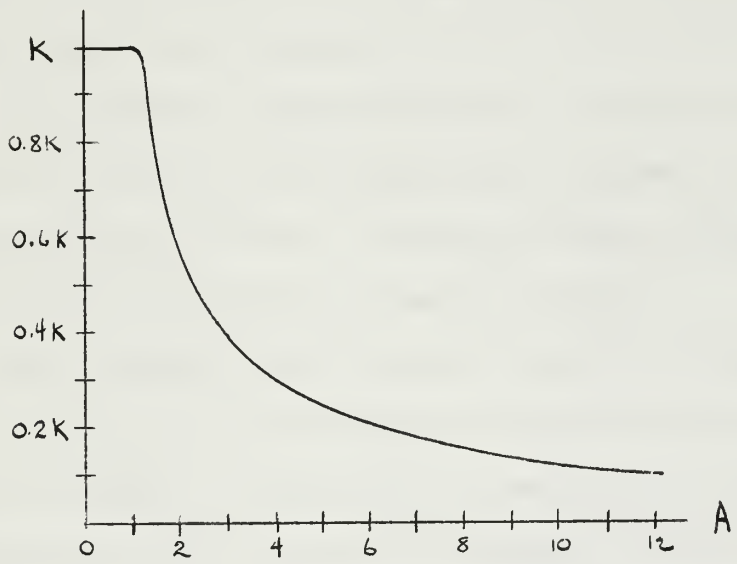

Figure 21

Describing Function of the Saturating Element

The describing function is useful in studying oscillation of the system when there is no input. A critical locus of $-\frac{1}{N(A)}$ can be plotted on the gain-phase plot of the open loop linear function. If this locus enters the region of instability for small values of A, an oscillation will grow until N(A) is reduced to the value at which the critical locus intersects the gain-phase plot of the open loop linear function.

If the amplitude of the oscillation increases further, the $-\frac{1}{N(A)}$ locus enters the region of stability and the oscillation is reduced in amplitude. Thus, in this illustration, the intersection of the $-\frac{1}{N(A)}$ locus and the gain-phase plot represent a point of stable oscillation at a frequency (from the gain-phase plot) and amplitude (from the critical locus) determined by the intersection.

This approach is justified because the linear elements of the system will filter out the high frequency components of the output of the non-linear element. The signal returned through the feedback loop will, therefore, be nearly sinusoidal.

The open loop, linear, transfer function of Figure 20 is plotted in the form of a Bode diagram in Figure 22 and on the gain-phase plane in Figure 23. The system is unstable as a result of the two integrations in the loop, and the critical locus will be entirely in the region of instability. The shape of the open loop function is

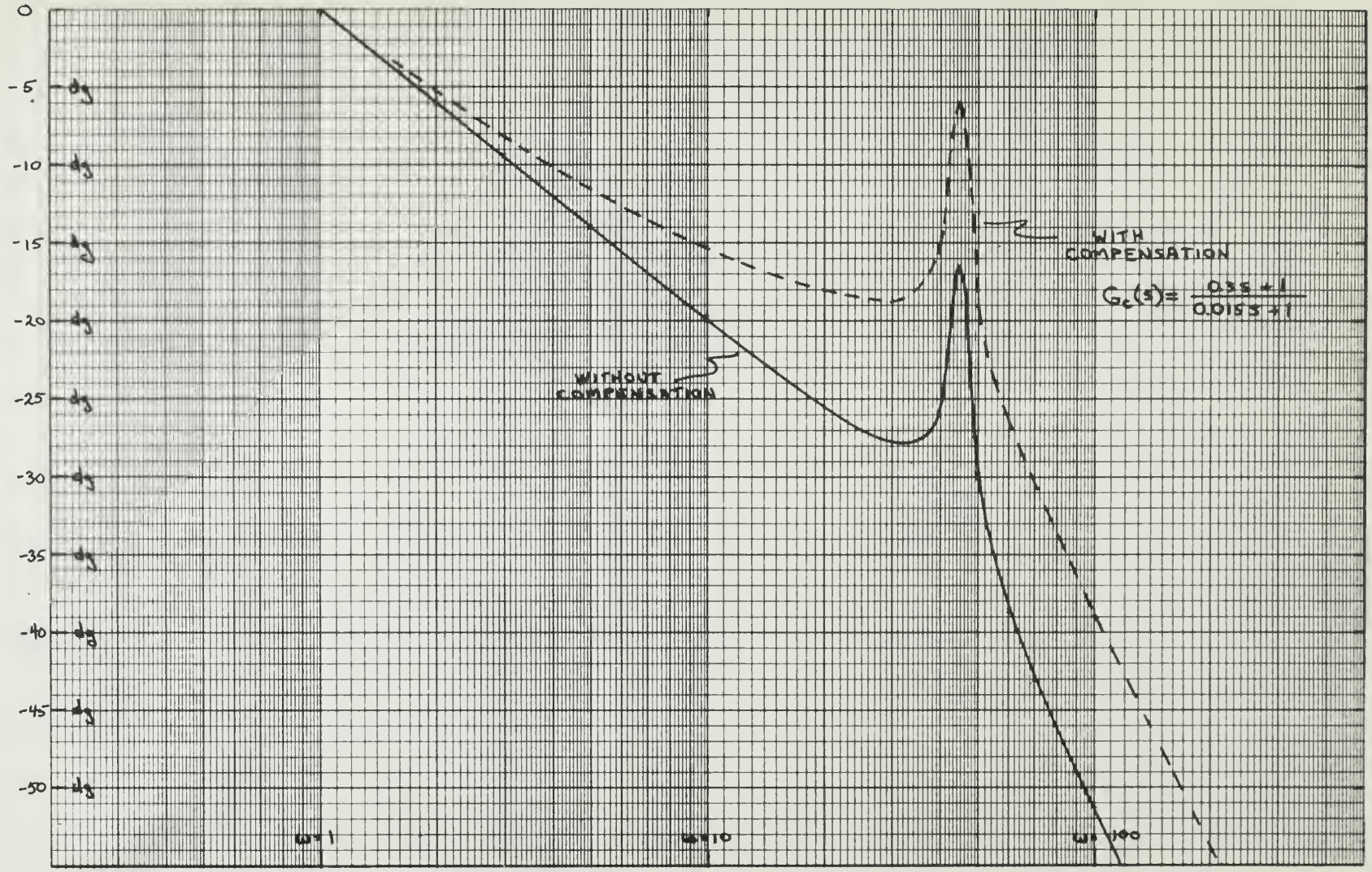

Figure 22(a) Bode Diagram of Open Loop Function (Magnitude)

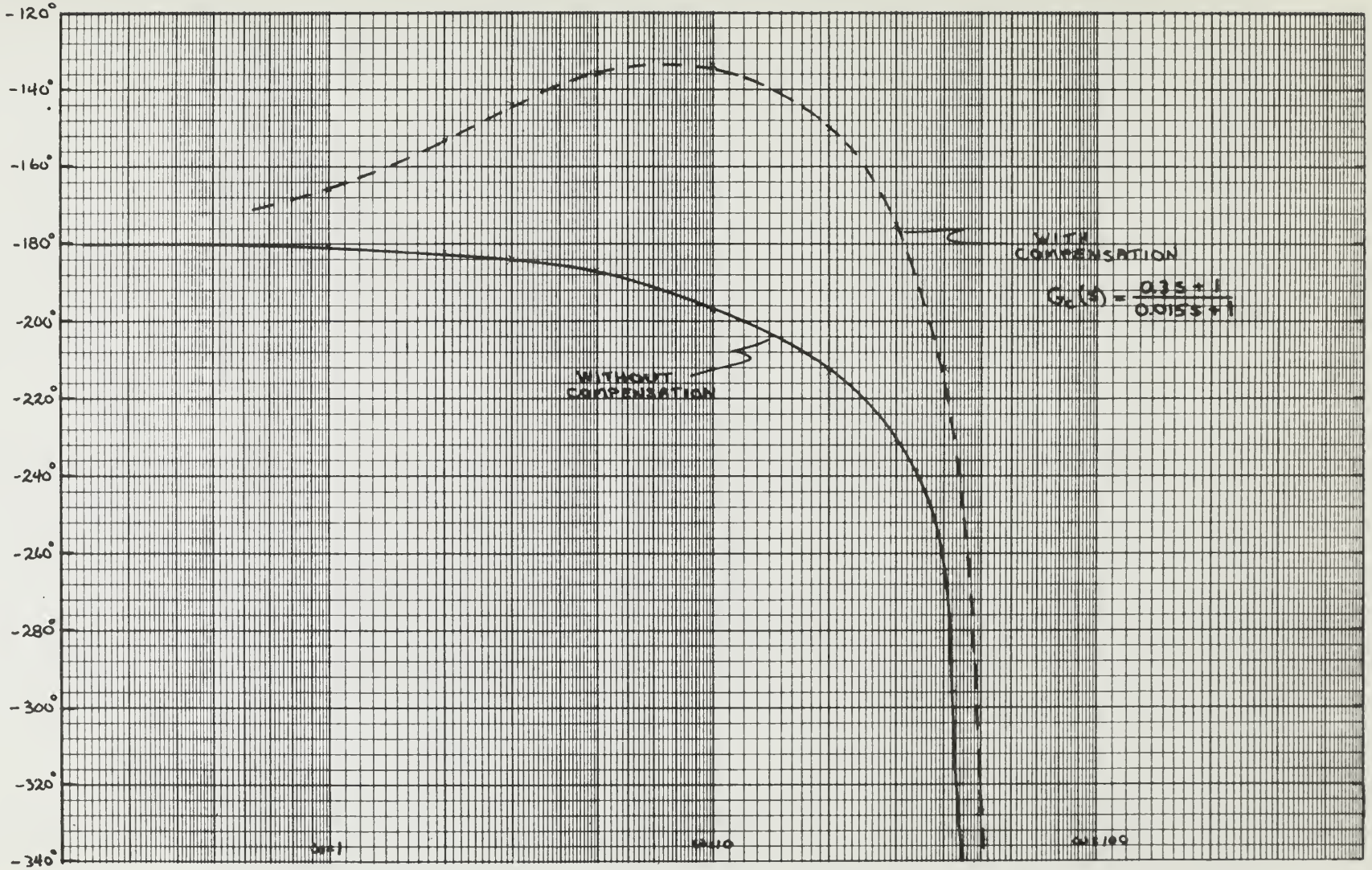

Figure 22(b) Bode Diagram of Open Loop Function (Angle)

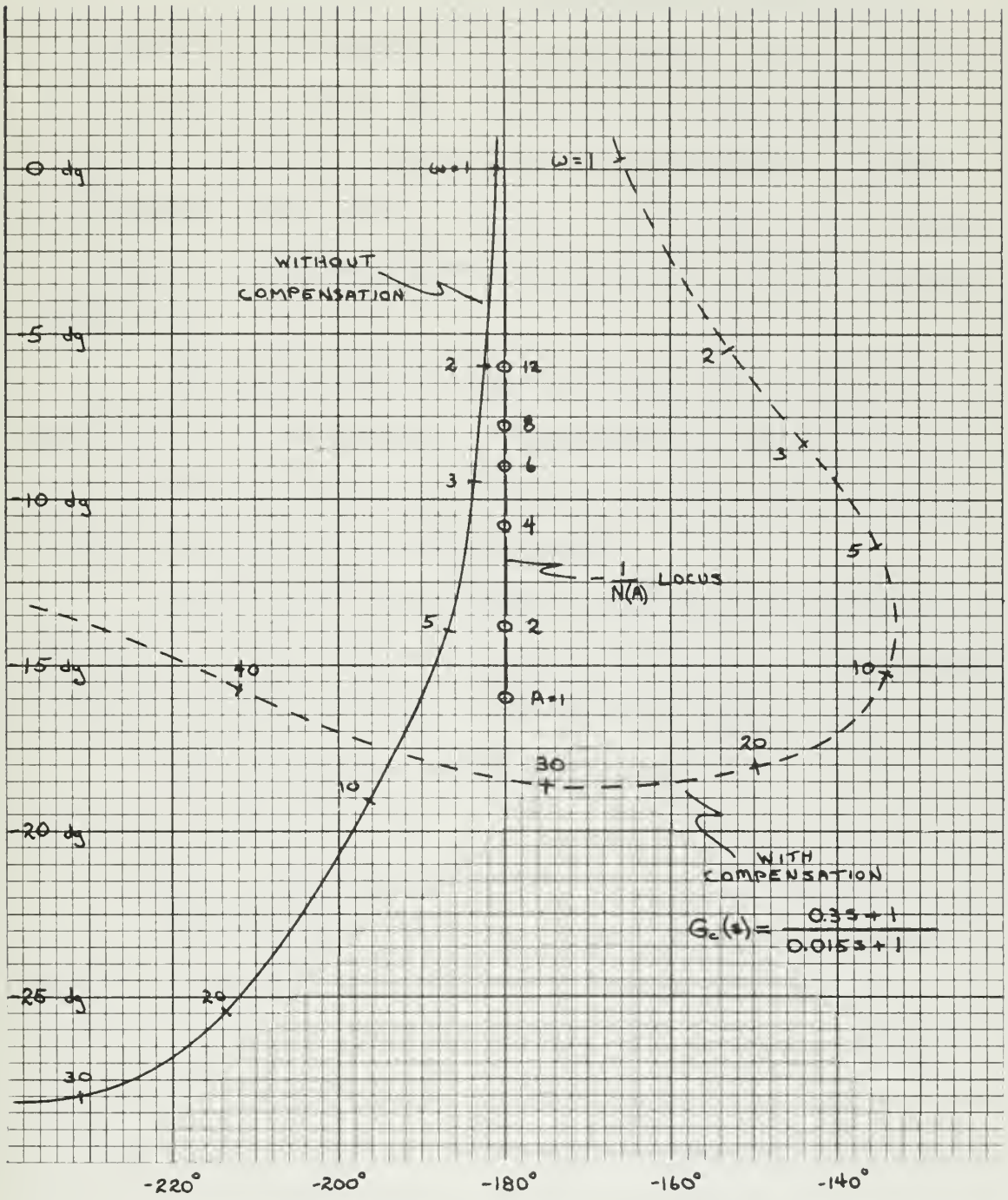

Figure 23

Gain-Phase Plot of Open Loop Function

altered by the addition of cascade compensation in the form of a lead network. The compensated open loop function is shown as a dashed line in the same figures. The system will be stable for an open loop gain less than 70. The value of K was set equal to 40, and the critical locus plotted in Figure 23. It is seen that the critical locus does not enter the region of instability, and stable oscillation cannot exist.

The response of the closed loop system will be dependent on amplitude as well as frequency. To judge the performance of the system, the responses to the test inputs described in Section II were obtained by putting the system on an analog computer.

The Philbrick Analog Computer in the Engineering Projects Laboratory, M. I. T., was used for the analysis. The computer diagram of Figure 24 was set up directly from the block diagram of Figure 19.

For the low speed range the test input is

$$x_S = .03 \sin 8t \text{ feet.}$$

The response to this input is shown in Figure 25, sketched from the oscilloscope presentation of the analog computer. Also shown is the DC motor torque and velocity. The performance of the system meets the specifications for this input. A step input of 0.5 foot was used to give an indication of the transient performance; the response is sketched in Figure 26 and is satisfactory.

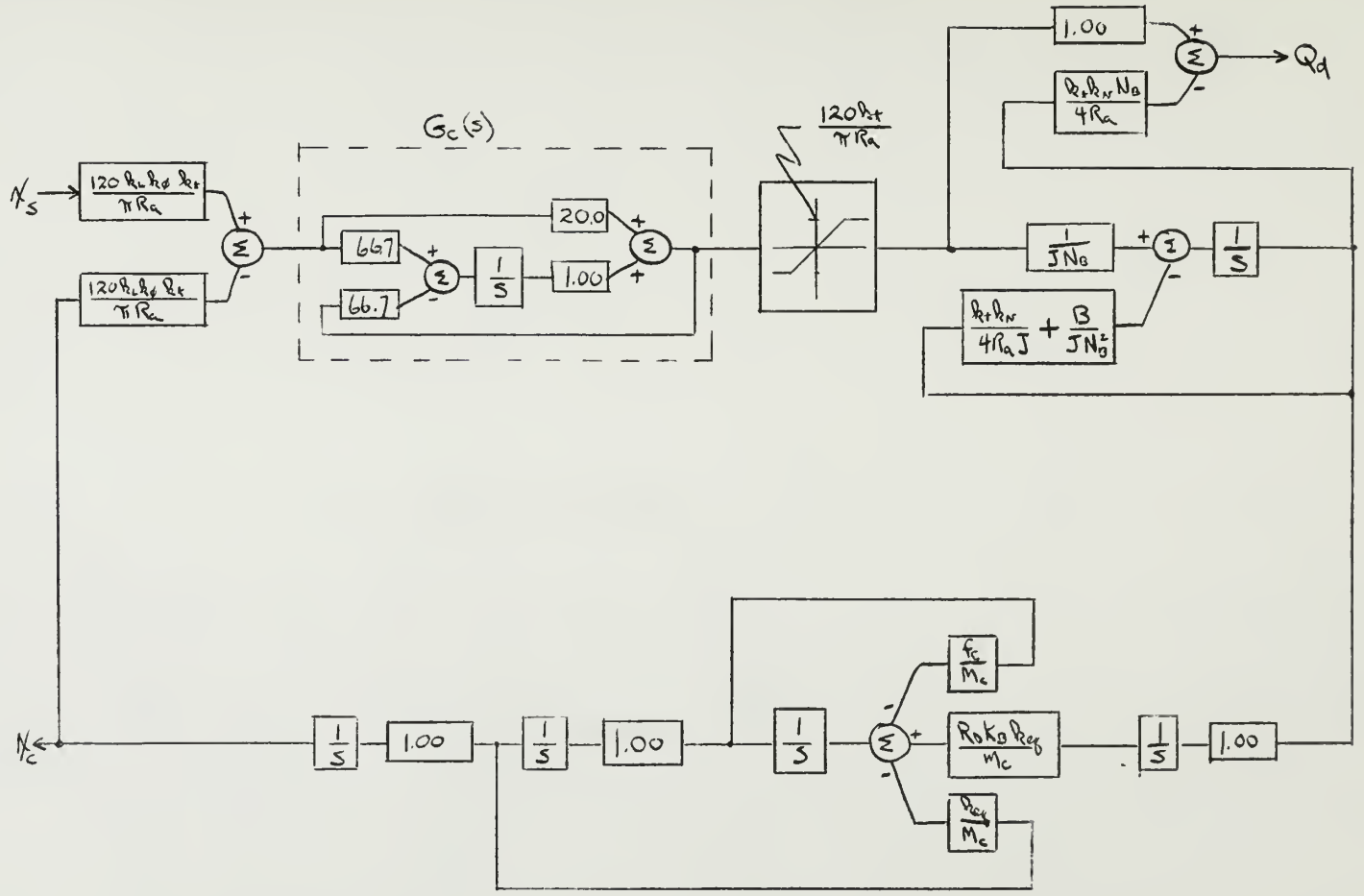

Figure 24

Analog Computer Diagram

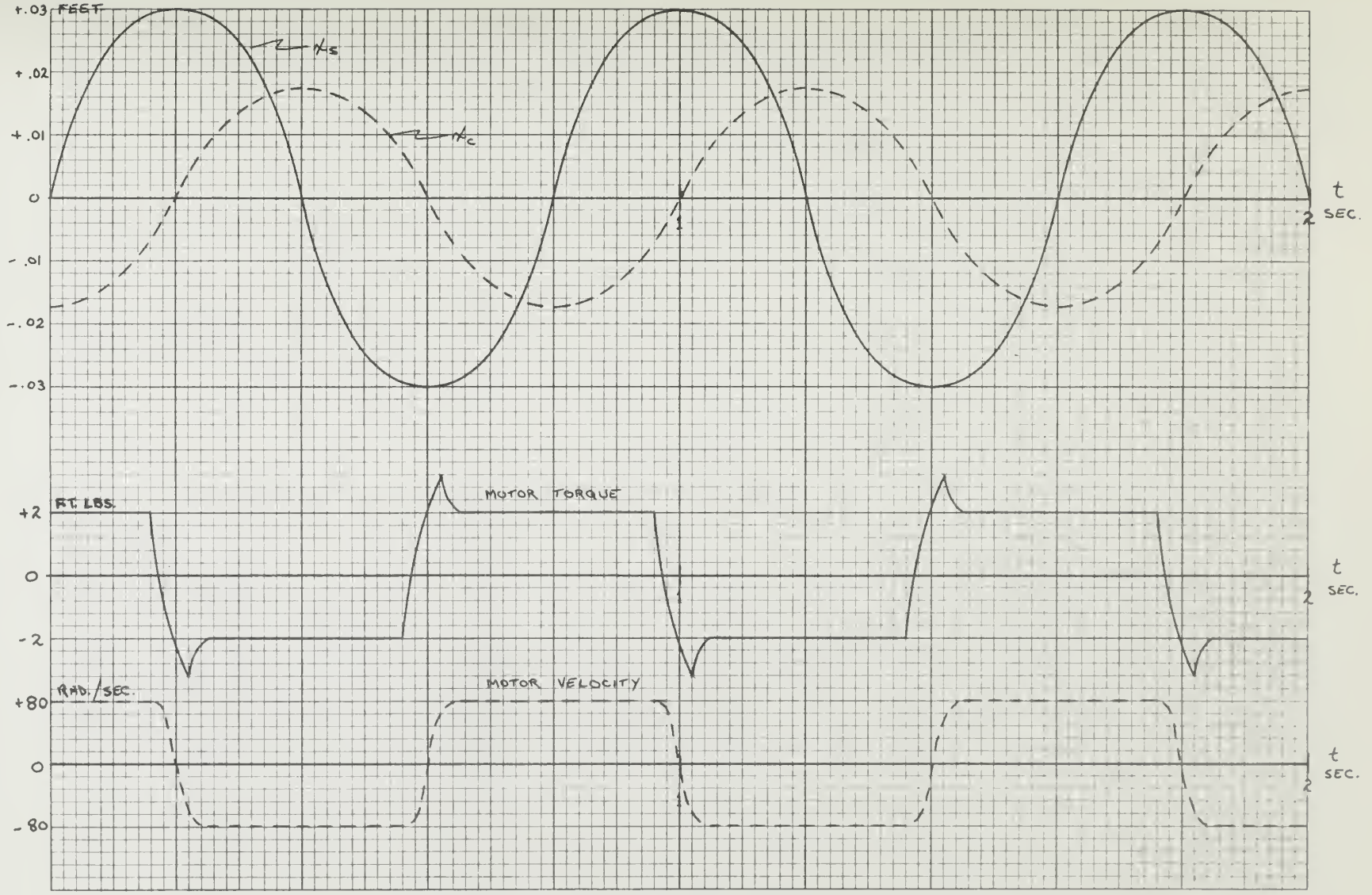

Figure 25 Response to Test Input x_s = .03 sin 8t feet

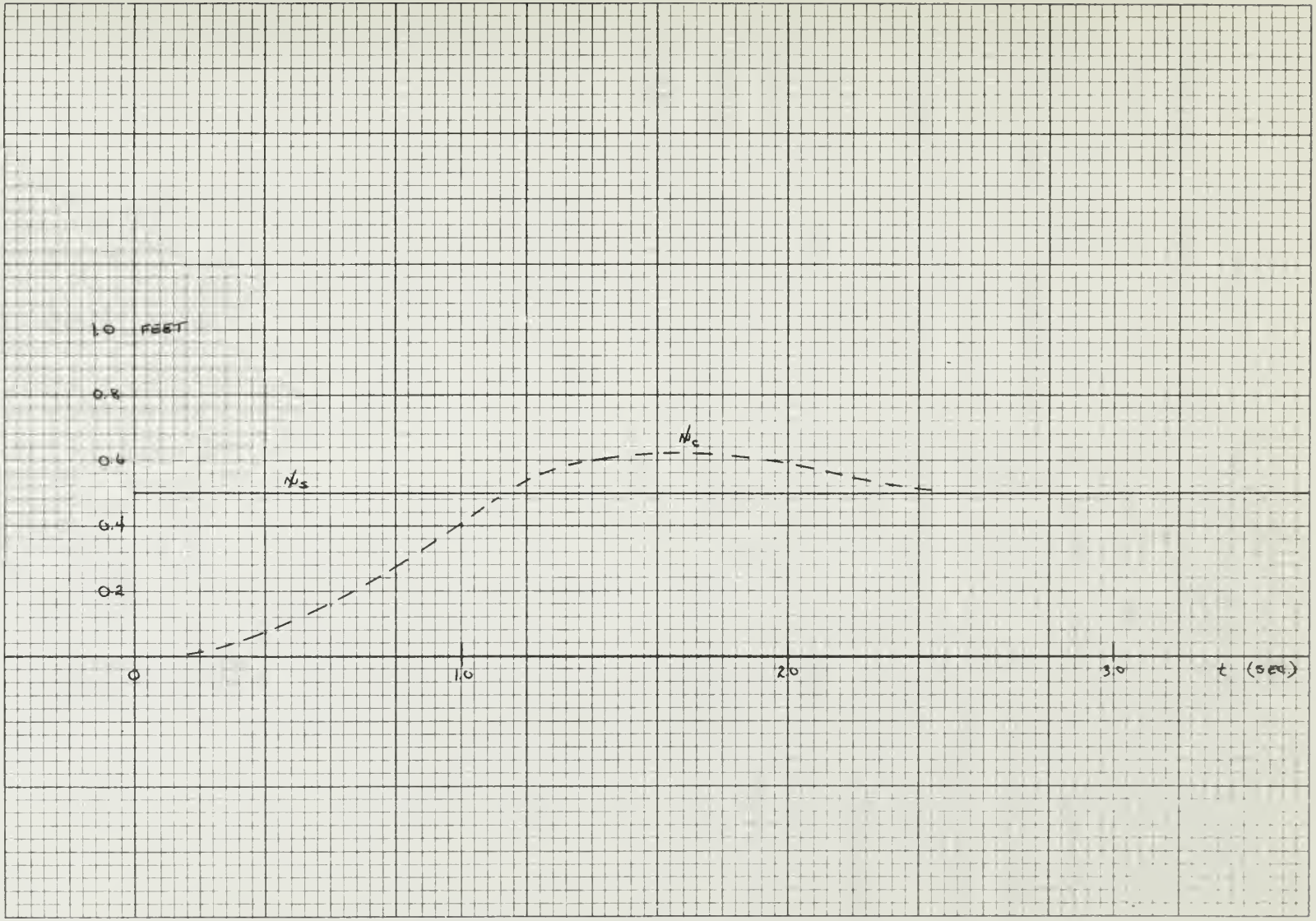

Figure 26 Response to Step Input of 0.5 feet

The test input for the system while in the high speed range is a ramp with a slope of 8.45 feet per second. Figure 27 shows the response, and it does not meet the specifications, the error exceeding four feet. The maximum value of the ramp for which the system can maintain the error less than one foot was determined to be 2.27 feet per second (Figure 28). This corresponds to a step change in model velocity of 2.27 feet per second or 1.34 knots.

It is evident from the DC motor torque and velocity curves sketched in Figure 27 that the velocity limitation of the control screw at 40 radians per second determined the system transient performance. The sketch also shows that there is little room for improvement.

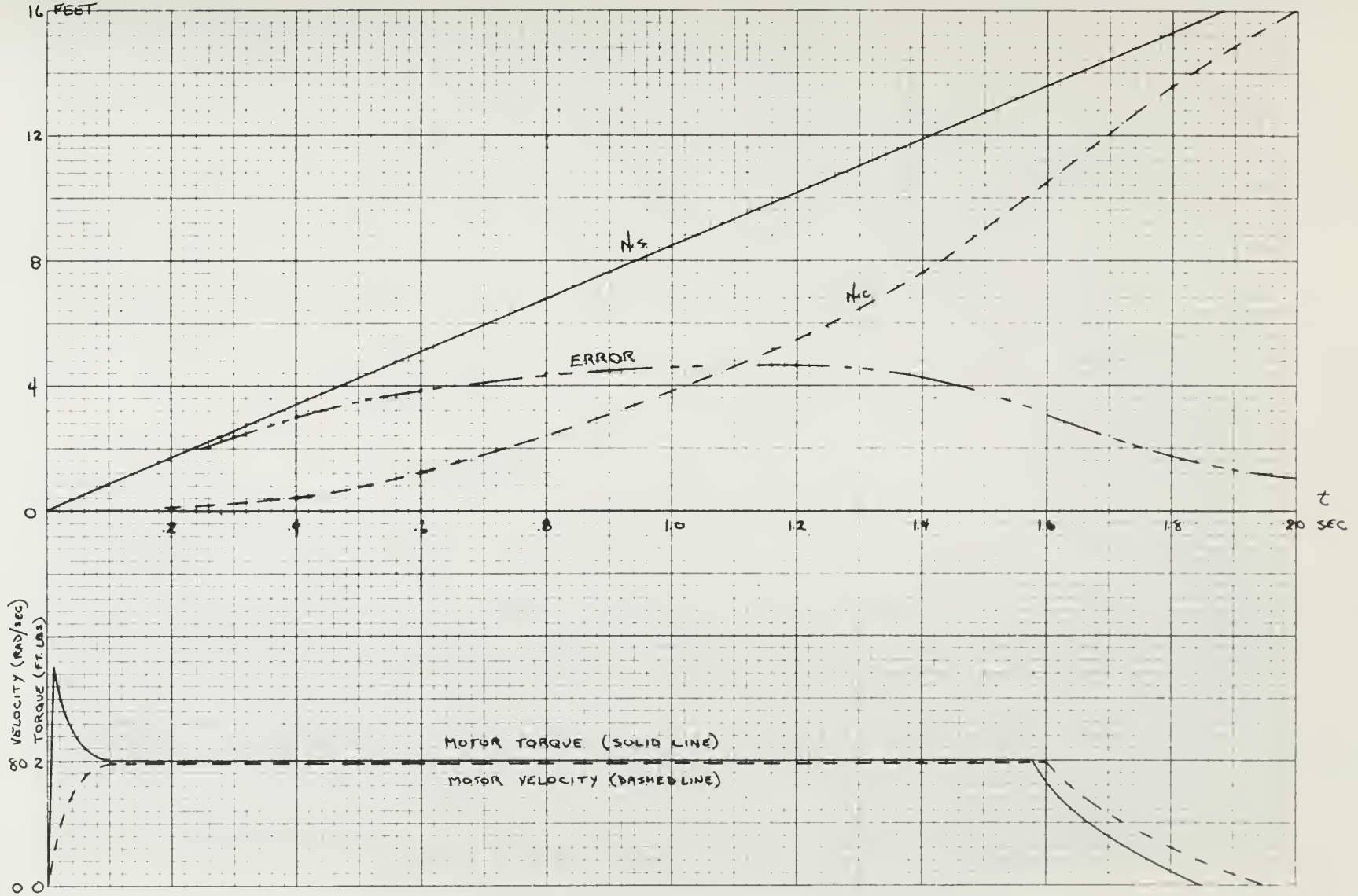

Figure 27 Response to Ramp Input of 8.45 feet per second

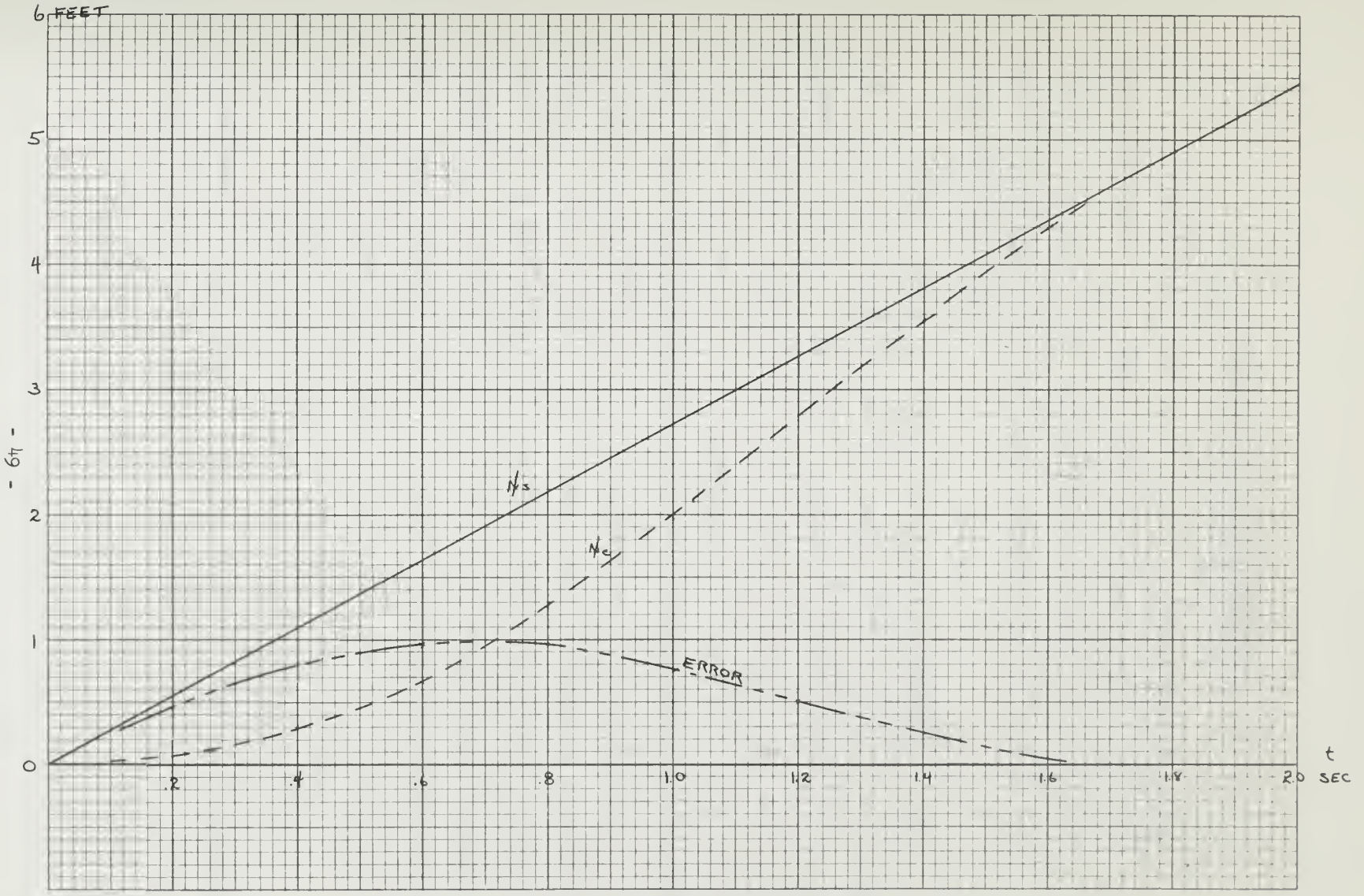

Figure 28 Response to Ramp Input of 2.27 feet per second

VII. CONCLUSIONS AND RECOMMENDATIONS

The system as designed meets all specifications except that to follow a model which undergoes a step change in velocity of 8.45 feet per second. The system is incapable of meeting this specification due to the velocity limitation of the control screw of the Link-Belt drive.

There are other factors which must be considered. The wire rope transmission has several undesirable features. This lightly damped second-order system will introduce vibrations which may interfere with model motions and with the instrumentation. The mechanical problems associated with the transmission have not been fully investigated. The drive sheave and idler must be located such that the span of wire rope not attached to the carriage does not interfere with carriage or model motions. This span should be supported at several points along the length of the tank to increase the spring constant. Foundations for the Link-Belt drive and the bearing supports for the drive sheave and idler must be provided. For high speed operation a step-up gear train between the Link-Belt unit and the drive sheave will be necessary. The damper must be added to the carriage.

All of the above make the system undesirable and the recommendation of the author is not to build it. The only justification for considering this system is the fact that the power element was available at no cost.

Placing a drive motor (electric or hydraulic) on the carriage eliminates the wire rope transmission and all its associated problems. The designer would then be free to select all the components and could build a system to meet the specifications. This approach has far greater potential than the one used in this design study and is recommended.

BIBLIOGRAPHY

1. Korvin-Kroukovsky, B. V., Theory of Seakeeping, The Society of Naval Architects and Marine Engineers, New York, 1961.

2. Vedeler, Georg , "Report on Seagoing Qualities of Ships," 7th International Conference on Ship Hydrodynamics, Publication No. 34 of the Swedish Ship Experimental Tank, Goteborg, Sweden, 1955, pp. 247-274.

3. Abkowitz, M. A., "Correlation of Model Tests in Waves - Report of Panel," 11th ATTC, David Taylor Model Basin, September 1956.

4. Sibul, O. J., "The Effect of Method of Towing on Ship Model Motions," University of California, Institute of Engineering Research, Series No. 61, Issue No. 13, June 1957.

5. Abkowitz, M. A., "An Analysis of Model Towing Conditions in Seakeeping Tests," Proc., Symposium of the Behavior of Ships in a Seaway, September 7-10, 1957, Wageningen, 1959.

6. Paulling, J. R., Jr., "Towing and Motion Measurement Instrumentation for Model Seakeeping Investigation," June 1956, presented to ATTC Session on Instrumentation and Facilities, DTMB, Sept. 1956.

7. Ben-Nun, Y. and Harel, J. E., "Seakeeping Tests of Series 60, Block 0.6 Ship Model," S.B. Thesis, M. I. T., Department of Naval Architecture and Marine Engineering, 1954.

8. Wiener, Z. B., "Report on Seakeeping Tests Done at the Towing Tank at M. I. T.," October 1958.

9. "Data for Aircraft Control Cables," American Chain and Cable Company, Inc., Bridgeport, Connecticut, 1951.

10. "P.I.V. Variable Speed Drives," Book No. 2274, Link-Belt Company, Pittsburg, Pennsylvania, 1950.

11. Newton, George C., Jr., "What Size Motor?" Machine Design, Nov. 1950.

12. Gibson, J. E. and Tuteur, F. B., Control System Components, McGraw-Hill Book Company, Inc., New York, 1958.

13. "G. E. Silicon Controlled Rectifier Manual," Third Edition, General Electric Company, New York, 1964.

14. Cantor, C., "Application of Silicon Controlled Rectifiers to a DC Servomotor," M. I. T. S.M. Thesis, August 1959.

15. Gille, J-C, Pélegrin, M. J. and Decaulne, P., Feedback Control Systems, McGraw-Hill Book Company, Inc., New York 1959.

16. Gibson, J. E., Nonlinear Automatic Control, McGraw-Hill Book Comapany, Inc., New York, 1963.

17. Higdon, A. and Stiles, W. B., Engineering Mechanics, Second Editions, Prentice-Hall, Inc., Englewood Cliffs, New Jersey, 1955.

18. "Rex Roller Chain Engineering, Catalog 720," Chain Belt Company, Milwaukee, Wis., 1962.

APPENDIX A

Weight of Carriage and Attachments

Weight of Basic Carriage* (Includes DC drive motor and gear box of present drive system)	254 pounds
Equipment	
Cross Brace	18.7 pounds
Electrical Equipment	6.5
Mounting Brackets	8.2
Equipment Total**	33.4 pounds
Attachments	
Surge Rig**	51.7 pounds
No-Surge Rig**	13.3
Yacht Test Rig**	69.2

Summary

Basic Carriage	254 pounds
Equipment	33
Surge Rig	52
TOTAL	339 pounds

Mass of Carriage Total = $\frac{339}{32.2}$ = 10.5 slugs

Approximate Mass Used for Design Purposes 10 slugs

*Accuracy $\pm$ 1 pound

**Accuracy $\pm$ 0.1 pound

APPENDIX B

Development of Incremental Linear Model for Spring Due to Catenary

Since the sag of the wire rope will be small compared to its length, its weight can be assumed to be distributed uniformly along the horizontal span instead of along the length of the wire without introducing an appreciable error. Under this assumption the shape will be a parabola[17]. The sag at the center when the ends are at the same level is given by

$$\epsilon = \frac{w\ell^2}{8H} \quad , \tag{1}$$

and for $\frac{\epsilon}{\ell} \ll \frac{1}{2}$ the approximate length of wire is

$$L = \ell + \frac{8\epsilon^2}{3\ell} \tag{2}$$

where L is the length of the wire

ℓ is the length of the span

ϵ is the sag at the center of the span

w is the weight per foot

H is the horizontal component of the tension

Substituting equation (1) into (2) yields

$$L = \ell + \frac{w^2 \ell^3}{24H^2} \tag{3}$$

For a constant length of wire the linear incremental model is developed as follows:

Let $\ell = \ell_0 + \Delta\ell$

$H = H_0 + \Delta H$

Substituting in equation (3) yields,

$$L = \ell_0 + \Delta\ell + \frac{w^2 \left(\ell_0^3 + 3\ell_0^2 \Delta\ell + 3\ell_0 \Delta\ell^2 + \Delta\ell^3\right)}{24\left(H_0^2 + 2H_0 \Delta H + \Delta H^2\right)} \tag{4}$$

Setting $\Delta\ell = 0$, $\Delta H = 0$ gives the equilibrium equation

$$L = \ell_0 + \frac{w^2 \ell_0^3}{24H_0^2} \quad . \tag{5}$$

Clearing fractions in equation (4) and subtracting the equilibrium equation (5) yields

$$2(L - \ell_0)\Delta H = \left(H_0 + \frac{w^2 \ell_0^2}{8H_0}\right) \Delta\ell \tag{6}$$

neglecting terms higher than first order.

From equation (5)

$$2(L - \ell_0) = \frac{w^2 \ell_0^3}{12 H_0^2} \quad . \tag{7}$$

Substituting (7) into (6) results in the desired relation for the spring constant

$$k_c = \frac{\Delta H}{\Delta \ell} = \frac{12 H_0^3}{w^2 \ell_0^3} + \frac{3 H_0}{2 \ell_0} \tag{8}$$

In this application the second term of equation (8) is small compared to the first and can be neglected. The final expression for the spring constant is then

$$k_c \approx \frac{12 H_0^3}{w^2 \ell_0^3}$$

Wire Rope Selection

As seen in Section III, it is desirable to have the natural frequency of the wire rope transmission system as high as possible; therefore, the equivalent spring constant must be as large as possible.

The spring constant of a wire stretched across a span will be that of a weightless, elastic spring acting in series with a non-elastic, weight-distributed cable with catenary. The relation for the first is given in Section III as

$$k_e = \frac{EA}{\ell_0} \quad ;$$

and that for the second is developed above as

$$k_c = \frac{12H_0^3}{w^2\ell_0^3}$$

The resultant, or equivalent, spring constant will be

$$k = \frac{k_e k_c}{k_e + k_c}$$

For high natural frequency both k_e and k_c must be large. For a given span, k_e increases with EA and, therefore, with increased diameter. The value of EA increases as the number of strands is

decreased; however, flexibility is lost. On the other hand, k_c is inversely proportional to w^2, but can be increased in direct proportion to H_o^3 within strength limitations.

The wire rope selected was $\frac{1}{4}$-inch, 1 x 19, stainless steel with the following properties:

breaking strength	8200 pounds
w	.135 pounds per foot
EA	853,500 pounds.

Roller chain was considered for the system, but it was found that it was heavier and more elastic for the same breaking strength as wire. The following data are given for comparison[18].

Chain No.	#35	#40
Pitch	3/8	1/2 inches
Width	3/16	5/16 inches
Breaking Strength	2100	3,700 pounds
w	0.22	0.41 pounds per foot
EA	113,000	201,000 pounds

Calculation of System Spring Constant

Because of the large inertia of the variable speed drive referred to the output shaft (Appendix C), the wire rope transmission system can be modeled as in Figure B1. The spans ℓ_1 and ℓ_2 will vary as the carriage moves down the tank with

$$\ell_1 + \ell_2 = 100 \text{ feet.}$$

The length ℓ_3 will remain constant at 100 feet. This length can be supported along its length without interference with carriage travel. The catenary effect will, therefore, be small; and only the elastic spring need be considered.

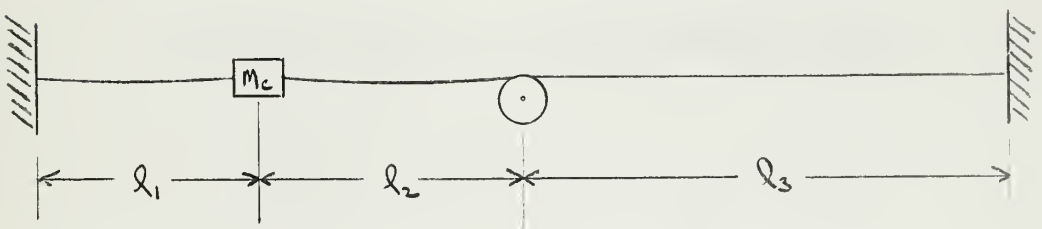

Figure B1
Model of Wire Rope Transmission System

The equivalent system is shown in Figure B2 with

$$k_1 = \frac{k_{e1} k_{c1}}{k_{e1} + k_{c1}}$$

where

$$k_{e1} = \frac{EA}{\ell_1}$$

$$k_{c1} = \frac{12 H_o^3}{w^2 \ell_1^3}$$

and

$$k_2 = \frac{k_{e2} k_{c2}}{k_{e2} + k_{c2}}$$

where

$$k_{e2} = \frac{EA}{\ell_2 + \ell_3}$$

$$k_{c2} = \frac{12 H_o^3}{w^2 \ell_2^3}$$

Finally the equivalent spring constant is given by

$$k_{eq} = k_1 + k_2 \quad .$$

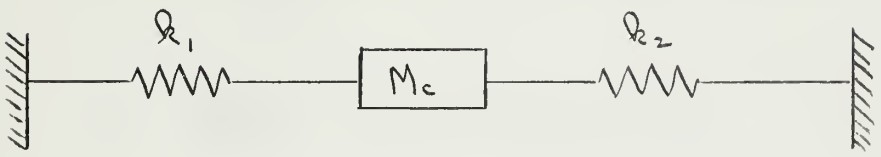

Figure B2
Equivalent Model

As noted previously the spring constant will vary as the carriage moves down the tank. To illustrate this effect the spring constant will be computed for three carriage positions:

Position	ℓ_1	ℓ_2
Start	80	20 feet
Mid-Run	50	50 feet
End	20	80 feet

For the wire selected with 400 pounds tension, the spring constant at each position is computed below.

$$k_{e1} = \frac{853500}{80} = 10{,}700 \text{ pounds per foot}$$

$$k_{c1} = \frac{12\ (400)^3}{(.135)^2(80)^3} = 82{,}200 \text{ pounds per foot}$$

$$k_1 = \frac{10{,}700 \times 82{,}200}{92{,}900} = 9470 \text{ pounds per foot}$$

$$k_{e2} = \frac{853500}{120} = 7{,}100 \text{ pounds per foot}$$

$$k_{c2} = \frac{12\ (400)^3}{(.135)^2(20)^3} = 5.27 \times 10^6 \text{ pounds per foot}$$

$$k_2 = \frac{7100 \times 5.27 \times 10^6}{5.27 \times 10^6} = 7{,}100 \text{ pounds per foot}$$

$$k_{eq} = k_1 + k_2$$

$$k_{eq} = 16{,}570 \text{ pounds per foot}$$

Mid-Run Position

$$k_{e1} = \frac{853500}{50} = 17{,}070 \text{ pounds per foot}$$

$$k_{c1} = \frac{12(400)^5}{(.135)^2(50)^3} = 337{,}000 \text{ pounds per foot}$$

$$k_1 = \frac{17{,}070 \times 337{,}000}{354{,}000} = 16{,}200 \text{ pounds per foot}$$

$$k_{e2} = \frac{853500}{150} = 5{,}690 \text{ pounds per foot}$$

$$k_{c2} = \frac{12\ (400)^3}{(.135)^2(50)^3} = 337{,}000 \text{ pounds per foot}$$

$$k_2 = \frac{5{,}690 \times 337{,}000}{342{,}690} = 5{,}600 \text{ pounds per foot}$$

$$k_{eq} = k_1 + k_2$$

$$k_{eq} = 21{,}800 \text{ pounds per foot}$$

End Position

$$k_{e1} = \frac{853500}{20} = 42{,}680 \text{ pounds per foot}$$

$$k_{c1} = \frac{12\ (400)^3}{(.135)^2(20)^3} = 5.27 \times 10^6 \text{ pounds per foot}$$

$$k_1 = \frac{42{,}680 \times 5.27 \times 10^6}{5.31 \times 10^6} = 42{,}400 \text{ pounds per foot}$$

$$k_{e2} = \frac{853500}{180} = 4{,}740 \text{ pounds per foot}$$

$$k_{c2} = \frac{12\ (400)^3}{(.135)^2(80)^3} = 82{,}200 \text{ pounds per foot}$$

$$k_2 = \frac{4{,}740 \times 82{,}200}{86{,}940} = 4{,}480 \text{ pounds per foot}$$

$$k_{eq} = k_1 + k_2$$

$$k_{eq} = 46{,}900 \text{ pounds per foot}$$

The natural frequency of the transmission will be

$$\omega_n = \sqrt{\frac{k_{eq}}{M_c}}$$

where M_c is the mass of the carriage (10 slugs). Table B1 gives a summary of spring constants and natural frequencies at each position.

Table B1
Summary of Spring Constants
and Natural Frequencies

Position	k_{eq} (pounds per foot)	ω_n (radians per second)
Start	16,570	40.7
Mid-Run	21,800	46.2
End	46,900	68.5

For design purposes k_{eq} is taken as 20,000 pounds per foot which gives a natural frequency of 44.7 radians per second.

APPENDIX C

Link-Belt P.I.V. Drive Name Plate Data

Order No. L-I-62240A
Part No. 1170Y3-D
Size HMDG - 2
Input RPM 860
Ratio 4
H.P. Delivered at Output RPM
4.5 H.P. @ 124 RPM
2.3 H.P. @ 31 RPM

GE Triclad Induction Motor Name Plate Data

Model No. 5K254E882
Nema Class B Design
Type K
Code H
Frame 254
5 H.P.
3 Phase 60 CPS 220/440 Volts
Fl. Amp. 12.5/6.25
Fl. Speed 1750 RPM
Link-Belt Part No. 862Z1-6
GE No. ZH1609

Inertia of Variable Speed Drive Components

Component	Inertia (slug-feet^2)
Induction Motor	.0267
Input Gears (2:1 Reduction)	
Pinion	.000311
Gear	.00528
1st Reduction Output (2.78:1)	
Pinion	.0001865
Gear	.00802
2nd Reduction Output (5:1)	
Pinion	.0001865
Gear	.0494
P.I.V. Drive (Referred to Constant Speed Shaft)	
At Max. Output Speed	.0472
At Mean Output Speed	.0229
At Min. Output Speed	.0145
Total Inertia (Referred to Output Shaft)	
At Max. Output Speed	6.25
At Mean Output Speed	23.8
At Min. Output Speed	95.5
Control Screw	6.82×10^{-6}

APPENDIX D

Description of DC Servomotor

GE DC Servomotor, 4 pole, Permanent Magnet Field Frame 5BBY29YA (foot mounted)

1/4 H.P., 1140 RPM, Torque 1.151 foot-pounds
115 volts, 2.3 amperes
Armature resistance, R_a = 6.8 ohms

Armature inductance, L_a = 0.040 henries

Peak torque, T_m = 8.5 foot-pounds

Torque constant, k_t = 0.60 foot-pounds per ampere

Voltage constant, k_v = 0.83 volt-second per radian

Inertia of rotor, J_m = .00108 slug-feet^2

$$\tau_m = \frac{v_m J_m}{T_m} = 0.0151 \text{ seconds}$$

$$P_m = v_m T_m = 1010 \text{ foot-pounds per second}$$

Load Specifications

J_L = 6.82 x 10^{-6} slug-feet^2 (from Appendix C)

v_L = 40 radians per second (from Figure 7, Section IV)

α_L = 400 radians per second^2

T_L = 4 foot-pounds

$$\tau_L = \frac{v_L}{\alpha_L} = 0.1 \text{ seconds}$$

$$P_L = v_L(J_L\alpha_L + T_L) = 160 \text{ foot-pounds per seconds}$$

Motor Selection Procedure

$$\frac{\tau_m}{\tau_L} = \frac{0.0151}{0.1} = 0.151$$

for $\frac{\tau_m}{\tau_L} \leq 1/2$

$$\frac{P_m}{P_L} \geq \frac{1}{1 - \frac{\tau_m}{\tau_L}}$$

$$\frac{1010}{160} \geq \frac{1}{1 - 0.151}$$

$$6.3 \geq 1.18$$

Motor selected is satisfactory.